DOT/FAA/PM-87-25

Project Report
ATC-147

TDWR PRF Selection Criteria

S. C. Crocker

15 March 1988

Lincoln Laboratory
MASSACHUSETTS INSTITUTE OF TECHNOLOGY
LEXINGTON, MASSACHUSETTS

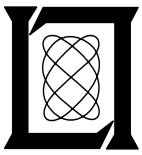

Prepared for the Federal Aviation Administration,
Washington, D.C. 20591

TECHNICAL REPORT STANDARD TITLE PAGE

1. Report No.	2. Government Accession No.	3. Recipient's Catalog No.
DOT/FAA/PM-87-25		

4. Title and Subtitle	5. Report Date
TDWR PRF Selection Criteria	15 March 1988
	6. Performing Organization Code

7. Author(s)	8. Performing Organization Report No.
Sandra C. Crocker	ATC-147

9. Performing Organization Name and Address	10. Work Unit No. (TRAIS)
Lincoln Laboratory, MIT P.O. Box 73 Lexington, MA 02173-0073	11. Contract or Grant No. DTFA-01-80-Y-10546
	13. Type of Report and Period Covered
12. Sponsoring Agency Name and Address Department of Transportation Federal Aviation Administration Program Engineering Service Washington, DC 20591	Project Report
	14. Sponsoring Agency Code

15. Supplementary Notes

The work reported in this document was performed at Lincoln Laboratory, a center for research operated by Massachusetts Institute of Technology, under Air Force Contract F19628-85-C-0002.

16. Abstract

The Terminal Doppler Weather Radar (TDWR) system shall provide high quality Doppler radar data on weather phenomena near high traffic airports. These data shall be used in real time by automated TDWR algorithms to detect weather situations which may be hazardous to the safe operation of aircraft within the vicinity of the airport.

One of the major factors which could cause the degradation of the qulity of these TDWR data is obscuration by "distant" storm cells. This obscuration is caused by storms located beyond the range interval being sampled by the radar, yet whose radar echo ambiguously folds within the range interval of interest. These range aliased echoes could trigger false detections by the algorithms, and/or cause actual hazardous situations near the airport to remain undetected.

By carefully selecting the pulse repetition frequency (PRF) of the radar, range obscuration from distant storms can be minimized over specified airport regions. This document describes techniques for predicting the obscuration as a function of PRF, and details the criteria which shall be used by the TDWR system to automatically and adaptively select an optimal PRF in order to minimize these obscuration effects.

17. Key Words		18. Distribution Statement
weather radar TDWR radar Pulse Repetition Frequency (PRF)	radar range obcuration radar range aliasing	Document is available to the public through the National Technical Information Service, Springfield, VA 22161.

19. Security Classif. (of this report)	20. Security Classif. (of this page)	21. No. of Pages	22. Price
Unclassified	Unclassified	66	

FORM DOT F 1700.7 (8-69)

ABSTRACT

The Terminal Doppler Weather Radar (TDWR) system shall provide high quality Doppler radar data on weather phenomena near high traffic airports. These data shall be used in real time by automated TDWR algorithms to detect weather situations which may be hazardous to the safe operation of aircraft within the vicinity of the airport.

One of the major factors which could cause the degradation of the quality of these TDWR data is obscuration by "distant" storm cells. This obscuration is caused by storms located beyond the range interval being sampled by the radar, yet whose radar echo ambiguously folds within the range interval of interest. These range aliased echoes could trigger false detections by the algorithms, and/or cause actual hazardous situations near the airport to remain undetected.

By carefully selecting the pulse repetition frequency (PRF) of the radar, range obscuration from distant storms can be minimized over specified airport regions. This document describes techniques for predicting the obscuration as a function of PRF, and details the criteria which shall be used by the TDWR system to automatically and adaptively select an optimal PRF in order to minimize these obscuration effects.

TABLE OF CONTENTS

Abstract	iii
List of Illustrations	vii
1.0 Introduction	1
1.1 Range Ambiguities	1
1.2 Radial Velocity Ambiguities	1
1.3 Simultaneous Range and Radial Velocity Measurements	2
1.4 TDWR Requirements	3
2.0 Statement of Problem	5
2.1 Required Airport Coverage	5
2.2 Definition of Distant Weather	5
2.3 Determination of Obscuration	6
2.4 Minimization of Obscuration	7
2.5 Prediction of Obscured Regions	7
3.0 Obscuration Minimization Criteria	9
3.1 Locations of Interest	9
3.1.1 General Areas	9
3.1.2 Meteorological Areas	9
3.1.3 Runway Areas	9
3.1.4 Meteorologically Active Runway Areas	9
3.1.5 Miscellaneous Areas	10
3.2 Selection Criteria	10
3.2.1 Priority 1	10
3.2.2 Priority 2	10

3.2.3 Priority 3 10

3.2.4 Priority 4 10

3.2.5 Statement of Selection Criteria 10

4.0 Sample Software Realization 15

4.1 Software Overview 15

4.2 TDWR Testbed Preliminaries 15

4.3 Performance Examples 17

4.3.1 Case 1: 12 to 13 June 1987 17

4.3.2 Case 2: 2 to 3 July 1987 24

4.3.3 Case 3: 15 August 1987 24

4.3.4 Case 4: 4 September 1987 37

5.0 Conclusion 49

Appendix A 51

Acknowledgment 55

References 57

LIST OF ILLUSTRATIONS

Figure No.		Page
1-1	Range Ambiguities	1
1-2	Simultaneous Unambiguous R_a and v_a Intervals	2
2-1	Obscuration vs PRF Value	6
3-1	An Example of the PRF Selection Criteria	14
4-1	Top Level Flow Diagram for PRF Algorithm	16
4-2	Reflectivity Profiles of 12 to 13 June 1987	19
4-3	Obscuration Assessment at 0107 UT	21
4-4	Gust Front Obscuration Profile at 0107 UT	21
4-5	Predicted Gust Front Obscuration at 0107 UT	21
4-6	Obscuration Profiles of 12 to 13 June 1987	23
4-7	Reflectivity Profiles of 2 to 3 July 1987	25
4-8	Obscuration Profiles of 2 to 3 July 1987	27
4-9	Obscuration Assessment at 0118 UT	29
4-10	Predicted Gust Front Obscuration at 0118 UT	29
4-11	Reflectivity Profiles of 15 August 1987	31
4-12	Obscuration Profiles of 15 August 1987	33
4-13	Obscuration Assessment at 2003 UT	35
4-14	Microburst Obscuration Profile at 2003 UT	35
4-15	Reflectivity Profiles of 4 September 1987	39
4-16	Distant Weather at 1849 UT	41
4-17	Microburst Region Obscuration Assessment at 1849 UT	41

4-18	Gust Front Region Obscuration Assessment at 1849 UT	43
4-19	Distant Weather at 2021 UT	45
4-20	Microburst Region Obscuration Assessment at 2021 UT	45
4-21	Gust Front Region Obscuration Assessment at 2021 UT	47
4-22	Range Aliased Returns at 2023 UT	47
A-1	Arc Distance vs Altitude	51
A-2	Growth Patterns of Storms of Varying Intensity	52
A-3	Percent of Cells Reaching an Altitude	53

1.0 Introduction

1.1 Range Ambiguities

The range interval, R_a , over which data from a pulsed radar may be collected unambiguously is easily calculated [1] if the time between pulses, T_p, is known; i.e.,

$$R_a = c \frac{T_p}{2} \text{ , where } c \text{ is the speed of light.}$$

Objects which are located beyond R_a, but which may be large enough to cause the return of the radar echo, will actually appear at a range less than or equal to R_a, as illustrated in Fig. 1-1. In Fig. 1-1a, three objects, labelled A, B, and C, are each located some distance from the radar. Because the sampling interval, T_p , is sufficiently large, the locations of A, B, and C can be deduced unambiguously from their returned echoes. When the sampling interval is significantly reduced, however, to say, T_p' , the echo returns of B and C ambiguously fold into the newly derived R_a', as seen in Fig. 1-1b. These range aliased echoes can obviously obscure the data which are being collected within the R_a' interval. To deal exclusively with the problem of minimizing range ambiguities, T_p would be *increased* until its corresponding R_a interval encompasses the ranges of all anticipated objects.

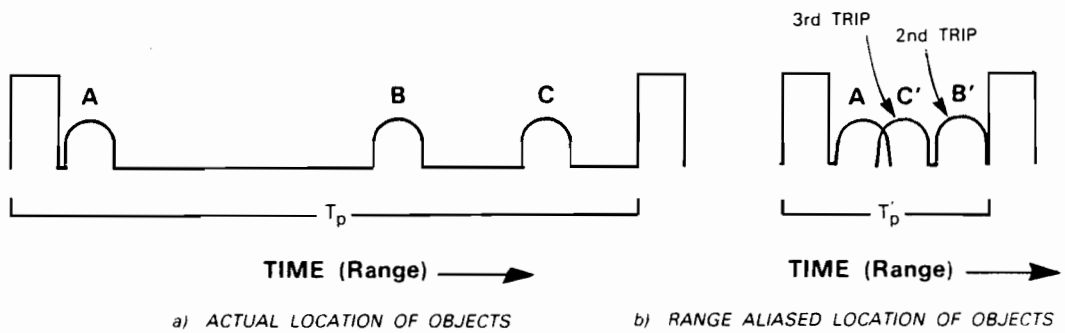

Figure 1-1. Range ambiguities.

1.2 Radial Velocity Ambiguities

Radial velocity (sometimes referred to as Doppler) radar measurements are obtained by analyzing the coherent phase changes of radar echoes over time. The interval over which radial velocity data may be collected unambiguously, v_a, can be calculated [1] if the radar wavelength, λ , and the time between pulses, T_p , is known: i.e.,

$$v_a = (+/-) \frac{\lambda}{4T_p} \text{ , where + and - indicate velocities away from and toward the radar, respectively.}$$

Data obtained on an object which is traveling at a radial velocity outside the v_a interval will appear aliased in velocity: i.e., the object will actually appear to be traveling at some

reduced velocity which lies within the v_a interval. To deal exclusively with the problem of minimizing radial velocity ambiguities, T_p would be *decreased* until its corresponding v_a interval is sufficiently large to encompass the radial velocities of all anticipated objects under investigation.

1.3 Simultaneous Range and Radial Velocity Measurements

Certain situations require the collection of both unambiguous range and unambiguous radial velocity measurements. To simultaneously collect both types of data, under the constraint of a specified radar wavelength, tradeoffs associated with the time between pulses, or equivalently the pulse repetition frequency of the radar, occur, as illustrated in Fig. 1-2. This figure plots R_a versus v_a for several sample radar frequencies, namely, a 3 GHz S-Band and a 5.6 GHz C-Band. An example of the use of this figure is shown. A PRF of 1650 Hz (R_a = 90 km) is highlighted to demonstrate the resultant unambiguous velocity intervals, +/- 41 m/s and +/- 22 m/s, which are readily achievable for the S-Band and the C-Band radar, respectively.

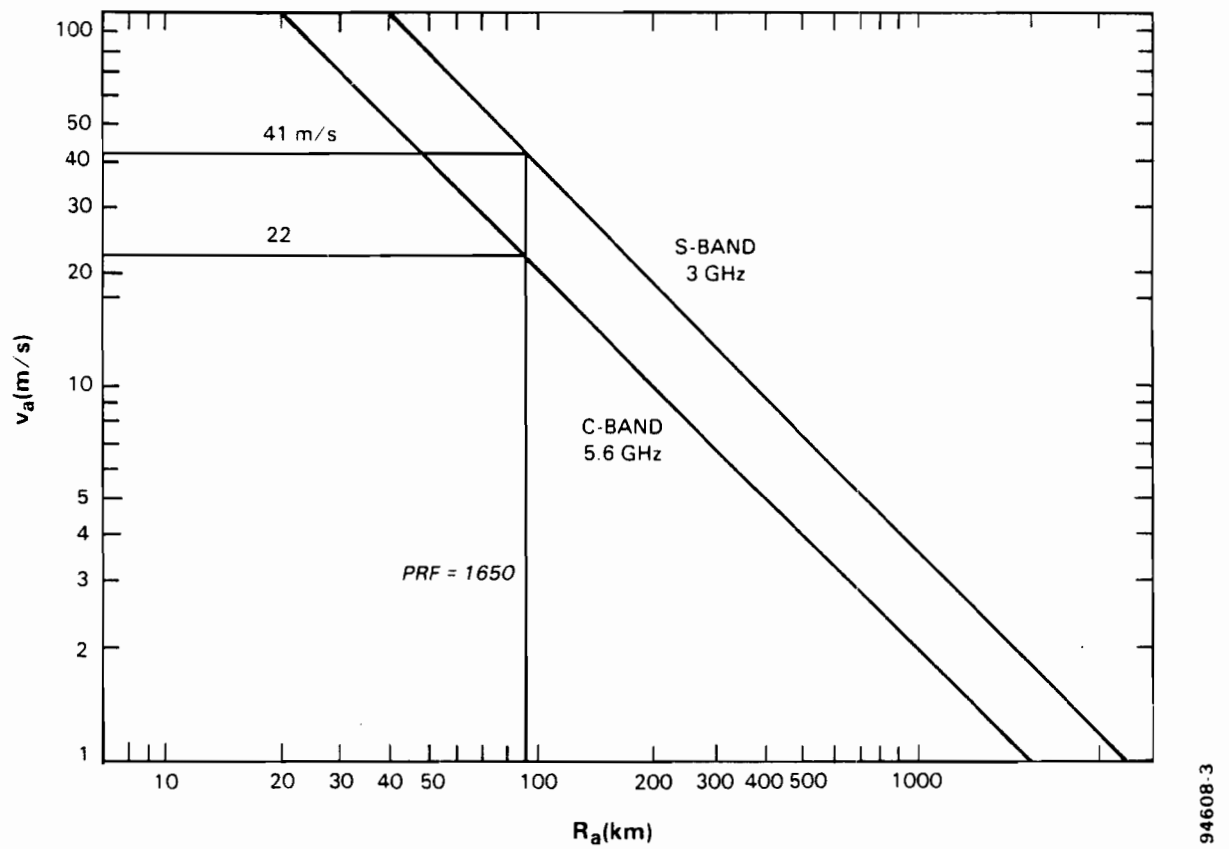

Figure 1-2. Simultaneous unambiguous R_a and v_a intervals.

1.4 TDWR Requirements

According to [2], the TDWR system shall operate at C-Band, shall obtain data out to ranges of at least 48 nmi (89.0 km), and shall obtain radial velocity data from -40 m/s to +40 m/s. By referring to the above figure, one clearly sees that these requirements for both unambiguous range and unambiguous radial velocity measurements cannot be met at C-Band by simple choice of PRF.

The TDWR contractor has been instructed to provide the means for automatically selecting the PRF "to minimize obscuration within user specified range/azimuth sectors due to out-of-trip weather echoes". The contractor has also been instructed that "hardware/software techniques may be employed to mitigate the effects of velocity aliasing to provide this measurement range (+/-40 m/s)".

This document develops the PRF selection criteria to be used by the TDWR system to minimize range obscuration from out-of-trip weather echoes. Section 2 introduces the TDWR airport coverage regions, and then develops, in four steps, the fundamental concepts of the PRF selection process. These steps involve first the identification of the distant weather; second, the assessment of obscuration which will be attributed to the distant weather; third, the selection of the PRF values; and fourth, the generation of an obscuration map. Section 3 defines the obscuration minimization criteria which leads to the PRF selection. Section 4 discusses the software realization of an automated and adaptive algorithm which is currently being tested for the obscuration mitigation task, and Section 5 concludes the report.

2.0 Statement of Problem

2.1 Required Airport Coverage

Two regions about the airport have been identified which must be examined by the TDWR system for the occurrence of hazardous weather, namely, the microburst region (also called the hazardous wind shift region) and the gust front region. As specified in [2], the microburst region is contained within a 6 nmi (11.1 km) radius about the airport, and is that region in which the automated TDWR microburst identification algorithm will operate. The automated gust front algorithm will operate on data which have been collected within a 40 nmi (74.1 km) radius [2] about the airport. These are the regions in which it is of utmost importance to ensure that the highest possible quality of data be collected. Within the scope of this report, these are the regions in which to minimize the effects of range obscuration from distant weather.

The minimization strategy is based on the assumption that a TDWR, which will typically be located approximately 15 km off-airport [3], shall be capable of operating at more than one PRF value. According to [2], the TDWR system shall collect high quality Doppler data using a PRF which has been chosen from a set of predetermined PRF values. In order to enable obscuration mitigation techniques to be employed, "the set of PRF values shall allow for at least a 50 km total variation in the basic unambiguous range interval, and consist of range increments of no greater that 3 km". This will result in the availability of more than one unambiguous range interval, and thus an ability to move distant weather obscuration about within the data gathering interval. Ideally, with the proper choice of PRF, range aliased weather returns will be placed over regions not requiring TDWR coverage for hazardous events.

Due to the fact that the two hazardous weather identification regions vary significantly in size, multiple PRF values will actually be selected and required for use.

2.2 Definition of Distant Weather

In order to support automatic and adaptive PRF selection, [2] defines a requirement to "produce quantitative reflectivity estimates out to an unambiguous range of at least 248 nmi" (460 km). This requirement is developed in Appendix A.

Distant weather shall be defined to be all regions about the radar which satisfiy three requirements: first, the returned signal strength (or reflectivity) associated with that region surpasses a site-dependent threshold value; second, the region is located beyond the minimum unambiguous range associated with the set of predetermined PRF values; and third, the region is located within 248 nmi of the radar.

According to [4], approximately once every five minutes, a low elevation distant weather surveillance scan will be conducted. The purpose of this scan is to identify the prevailing distant weather situation in order to subsequently assess range obscuration. The data from this scan are to be used to determine all regions which satisfy the above three requirements.

2.3 Determination of Obscuration

Once distant weather has been identified, obscuration from this weather to those areas which were specified in Section 2.1 can be determined as a function of PRF value. This calculation is illustrated in Fig. 2-1. Figure 2-1a first shows range from the radar versus some hypothetical set of PRF values. The curve labelled A illustrates the upper bound to the unambiguous range interval associated with each PRF value. Clearly, as the PRF value increases, the corresponding unambiguous range interval decreases. The subsequent curves on this figure bound regions from the radar which would fold into the unambiguous range interval on 2nd, 3rd, 4th, and possibly even 5th trip, depending on the selected PRF value.

As an example of the use of this graph in assessing obscuration as a function of PRF value, refer to Fig. 2-1b. Assume first that a point located 25 km from the radar is to remain free from out-of-trip range obscuration. If a storm, once again a point target, were identified 200 km from the radar, its 2nd trip return would fold onto the location to be protected if a PRF of 857 Hz were to be used. Its 3rd trip return would obscure the location if a PRF of 1714 Hz were to be used. Very simplistically, if either of those PRFs had been members of the TDWR "predetermined set" of available PRF values, they would not be selected for subsequent use. This example merely introduces the concept of obscuration avoidance. Since storms are not point targets, and since regions rather than points about the airport must be kept clear, the process of obscuration avoidance becomes more complex, as will be shown.

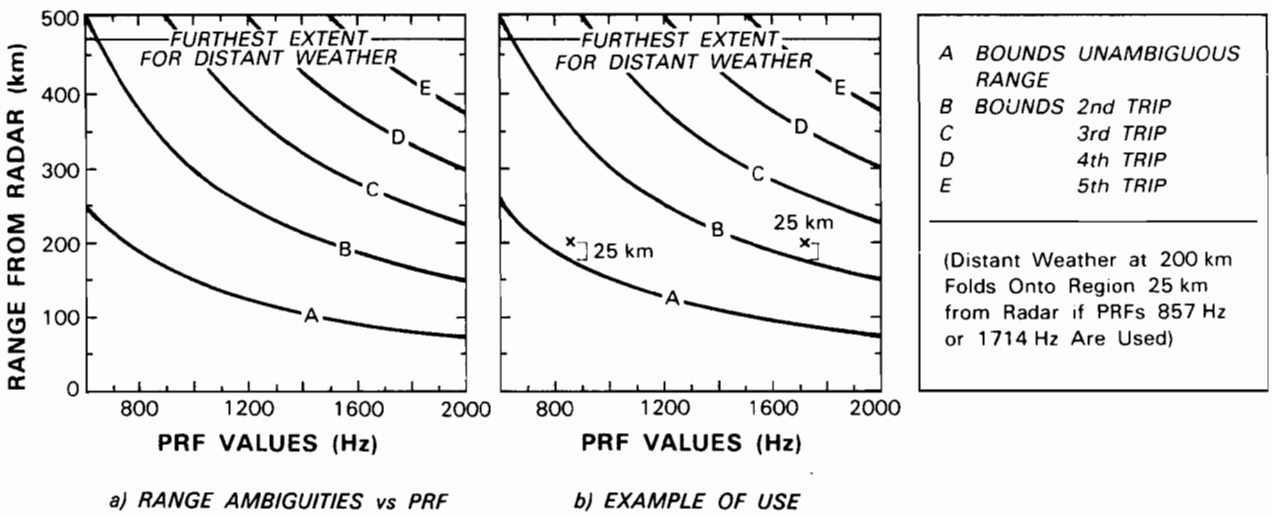

Figure 2-1. Obscuration vs PRF value.

2.4 Minimization of Obscuration

Using the low elevation surveillance scan, the TDWR shall periodically identify all distant weather. In a manner similar to that described above, all PRFs which would cause obscuration in the two hazardous weather identification regions are then determined. At the completion of the identification and obscuration assessment portions of the procedure, "optimal" PRFs are selected for subsequent use.

Ideally, there exists a PRF which results in no obscuration for the microburst region, and a PRF which results in no obscuration for the gust front region. Practical experience has demonstrated that this situation rarely occurs. Obscuration of some level will typically exist no matter what PRF is ultimately selected for use. The PRF selection process must include a means to assess "level" of obscuration, and then choose that PRF which shall result in the minimum level of obscuration. The minimization criteria to be used in the TDWR PRF selection process is described in Section 3.

2.5 Prediction of Obscured Regions

Once the optimal PRFs have been selected, any areas within the two hazardous weather regions, which will subsequently be obscured by range aliased echoes, must be identified. This obscuration information shall then be made available for use by the hazardous weather identification algorithms. The goal of this particular effort is to reduce the possibility of false alarms being triggered due to the presence of known range aliased data. A perceived radial velocity shear of sufficient strength to cause the declaration of a hazardous weather event, for example, may in fact be due to the mixing of radial velocity information from two different sources; i.e., an out-of-trip source with an in-trip source.

3.0 Obscuration Minimization Criteria

As was indicated, rarely does a situation exist in which the selected PRFs will result in totally obscuration free regions. Some degree of range obscuration will almost always exist within the hazardous weather identification regions. Where, within these regions, this obscuration falls is the concern of this section. Clearly, certain areas within each region should be considered more important than others to keep free from range contamination. Priorities of protection are therefore assigned to various locations within each of the two primary regions.

3.1 Locations of Interest

3.1.1 General Areas

One type of information that is to be computed by the PRF algorithm will profile the amount of out-of-trip obscuration by distant storm cells as a function of PRF value for each of the two general regions to be protected. This obscuration could be due to 2nd, 3rd, and possibly even 4th or 5th trip distant weather foldover (see Fig. 2-1), depending on the location of the distant storm(s) and the PRF used. The total area of obscuration which would be attributed to each available PRF value in these two general regions is to be calculated and retained for subsequent analysis.

3.1.2 Meteorological Areas

Range obscuration avoidance is to receive special attention on those areas which have been identified as either currently experiencing hazardous weather activity (e.g., microbursts or gust fronts) or possessing the potential to develop into hazardous weather activity (e.g., containing a microburst upper- or midlevel feature). These continually changing areas shall be periodically reported to the PRF selection algorithm from various meteorological algorithms within the TDWR system. The total area of obscuration over these meteorologically identified areas shall therefore be calculated and retained for subsequent analysis for each of the two regions of interest.

3.1.3 Runway Areas

Likewise, range obscuration avoidance is to receive special attention on active airport runway areas and up to 3 miles (4.8 km) away from runway thresholds along the extended runway centerline. These areas are site specific, and may periodically change, depending on which available runways are currently being used by airport traffic, and which are currently closed. Provisions shall therefore be made within the PRF algorithm to compute the total area of obscuration over these runway areas for each of the two regions of interest.

3.1.4 Meteorologically Active Runway Areas

It is of utmost importance to ensure that any location which is directly on the runways and which is experiencing or about to experience a potentially hazardous weather event be kept clear of any contamination due to out-of-trip weather. (This location would be the intersection of the two areas introduced in Sections 3.1.2 and 3.1.3.) Computations are to be made within the PRF algorithm to determine the total area of such

occurrence as a function of PRF value, and this information is to be retained for subsequent analysis.

3.1.5 Miscellaneous Areas

On rare occassion, a TDWR system may be situated in an area in which a second airport must be occassionally covered. In the event of this occurrence, it shall be possible for the PRF algorithm to determine obscuration as a function of PRF for specified regions about this second airport.

3.2 Selection Criteria

Information contained within the obscuration profiles associated with Section 3.1 will be combined to arrive at the optimal PRFs for use in the two regions under investigation. Ideally, all obscuration profiles for a region would achieve a minimum level of obscuration for the same PRF value, yet experience has shown that this is rarely the case. In the final determination of optimal PRF values, priorities must therefore be established which give the relative importance of obscuration minimization in each of the various areas introduced above.

3.2.1 Priority 1

It is of highest priority to minimize the area of obscuration on any portion of an active airport runway which has been identified as either experiencing, or perhaps about to experience, a hazardous meteorological event. This area of highest priority was introduced in Section 3.1.4.

3.2.2 Priority 2

The second highest priority shall be to minimize the area of obscuration on all active airport runways (those areas introduced in Section 3.1.2). This minimization, however, shall be subject to constraints imposed by Section 3.2.1.

3.2.3 Priority 3

The third highest priority shall be to minimize the area of obscuration over meteorologically identified areas, i.e., those areas introduced in Section 3.1.3. This minimization shall be subject to constraints imposed first by Section 3.2.1, and second, by Section 3.2.2.

3.2.4 Priority 4

The fourth and final priority shall be to minimize the area of obscuration within the general region under investigation. This area was introduced in Section 3.1.1. This minimization shall be subject to the contraints imposed first by Section 3.2.1, second, by Section 3.2.2, and third, by Section 3.2.3.

3.2.5 Statement of Selection Criteria

Using these established minimization priorities with the available obscuration profiles,

it is now possible to state the PRF selection procedure. This selection procedure is performed for obscuration profiles within both the microburst region and the gust front region.

The selection process first identifies a set of PRF values whose subsequent priority 1 obscuration level falls within an "acceptable" limit. From this set, priority 2 obscuration levels are examined to arrive at a subset of the previous set; i.e., a set which contains PRF values whose priority 2 obscuration levels fall within a second "acceptable" limit. This process is repeated until a fourth "acceptable" set is determined. From this final set, the optimal PRF is selected. In order to achieve the highest Nyquist interval, the highest PRF value within this set is selected for use. This can also be stated in terms of set theory notation as follows:

Let

region_1 be the previously identified microburst region
region_2 be the previously identified gust front region.

For $i = 1, 2$ let

$\mathbf{P1}_i$ be the total priority 1 area
$\mathbf{P2}_i$ be the total priority 2 area
$\mathbf{P3}_i$ be the total priority 3 area
$\mathbf{P4}_i$ be the total priority 4 area.

Further define

$\hat{\mathbf{P1}}_i$ as the set of obscured areas of $\mathbf{P1}_i$
$\hat{\mathbf{P2}}_i$ as the set of obscured areas of $\mathbf{P2}_i$
$\hat{\mathbf{P3}}_i$ as the set of obscured areas of $\mathbf{P3}_i$
$\hat{\mathbf{P4}}_i$ as the set of obscured areas of $\mathbf{P4}_i$.

Let the predetermined set of all TDWR PRF values be represented as **PRF** and define two sets, $\mathbf{PRF}_1$ and $\mathbf{PRF}_2$, to be equal to the set **PRF** , i.e.,

$$\mathbf{PRF} = \mathbf{PRF}_1 = \mathbf{PRF}_2.$$

Comment: We will select the PRF for the microburst region from $\mathbf{PRF}_1$ and the PRF for the gust front region from $\mathbf{PRF}_2$.

Consider functions $\mathbf{f}_i$, $\mathbf{g}_i$, $\mathbf{h}_i$, and $\mathbf{l}_i$, which map $\mathbf{PRF}_i$ into $\hat{\mathbf{P1}}_i$, $\hat{\mathbf{P2}}_i$, $\hat{\mathbf{P3}}_i$, and $\hat{\mathbf{P4}}_i$,respectively, according to the following notation:

$\mathbf{f}_i\ (PRF_{ij}) = \hat{P1}_{ij}$
$\mathbf{g}_i\ (PRF_{ij}) = \hat{P2}_{ij}$
$\mathbf{h}_i\ (PRF_{ij}) = \hat{P3}_{ij}$
$\mathbf{l}_i\ (PRF_{ij}) = \hat{P4}_{ij}$

where PRF_{ij} is any arbitrary element of $\mathbf{PRF}_i$, and $\hat{P1}_{ij}$, $\hat{P2}_{ij}$, $\hat{P3}_{ij}$, and $\hat{P4}_{ij}$ are elements of $\hat{\mathbf{P}}\mathbf{1}_i$, $\hat{\mathbf{P}}\mathbf{2}_i$, $\hat{\mathbf{P}}\mathbf{3}_i$, and $\hat{\mathbf{P}}\mathbf{4}_i$ respectively, and represent obscuration at PRF_{ij} .

Let $min\,1_i$ be defined such that

$min\,1_i = \mathbf{f}_i\ (PRF_{ik})$ for some PRF_{ik} in $\mathbf{PRF}_i$, and
$min\,1_i \leq \mathbf{f}_i\ (PRF_{il})$ for any arbitrary PRF_{il} in $\mathbf{PRF}_i$.

Comment: PRF_{ik} is that PRF within $\mathbf{PRF}_i$ which minimizes obscuration within the priority 1 area.

Let $par\,1_i$ be a pair of site adaptable parameters, and define the set $\mathbf{PRF}_i'$ such that $\mathbf{PRF}_i' \subseteq \mathbf{PRF}_i$, and for any arbitrary PRF_{im} in $\mathbf{PRF}_i'$,

$\mathbf{f}_i\ (PRF_{im}) \leq min\,1_i + par\,1_i$.

Comment : The set $\mathbf{PRF}_i'$ is all PRFs within $\mathbf{PRF}_i$ whose obscured priority 1 area is within $par\,1_i$ km^2 of the minimum.

Now let $min\,2_i$ be defined such that

$min\,2_i = \mathbf{g}_i\ (PRF_{in})$ for some PRF_{in} in $\mathbf{PRF}_i'$, and
$min\,2_i \leq \mathbf{g}_i\ (PRF_{ip})$ for any arbitrary PRF_{ip} in $\mathbf{PRF}_i'$.

Comment : PRF_{in} is that PRF within $\mathbf{PRF}_i'$ which minimizes obscuration within the priority 2 area.

Let $par\,2_i$ be a second pair of site adaptable parameters, and define the set $\mathbf{PRF}_i''$ such that $\mathbf{PRF}_i'' \subseteq \mathbf{PRF}_i'$, and for any arbitrary PRF_{iq} in $\mathbf{PRF}_i''$,

$\mathbf{g}_i\ (PRF_{iq}) \leq min\,2_i + par\,2_i$.

Comment : The set $\mathbf{PRF}_i''$ is all PRFs within $\mathbf{PRF}_i'$ whose obscured priority 2 area is within $par\,2_i$ km^2 of the minimum.

Let $min\,3_i$ be defined such that

$min\,3_i = \mathbf{h}_i\ (PRF_{ir})$ for some PRF_{ir} in $\mathbf{PRF}_i''$, and
$min\,3_i \leq \mathbf{h}_i\ (PRF_{is})$ for any arbitrary PRF_{is} in $\mathbf{PRF}_i''$.

Comment : PRF_{ir} is that PRF within $\mathbf{PRF}_i''$ which minimizes obscuration within the priority 3 area.

Let $par3_i$ be a third pair of site adaptable parameters, and define the set $\mathbf{PRF}_i'''$ such that $\mathbf{PRF}_i''' \subseteq \mathbf{PRF}_i''$, and for any arbitrary PRF_{it} in $\mathbf{PRF}_i'''$,

$$\mathbf{h}_i\ (PRF_{it}) \leq min3_i + par3_i\ .$$

Comment : The set $\mathbf{PRF}_i'''$ is all PRFs within $\mathbf{PRF}_i''$ whose obscured priority 3 area is within $par3_i$ km^2 of the minimum.

Finally, let $min4_i$ be defined such that

$min4_i = \mathbf{l}_i\ (PRF_{iu})$ for some PRF_{iu} in $\mathbf{PRF}_i'''$, and
$min4_i \leq \mathbf{l}_i\ (PRF_{iv})$ for any arbitrary PRF_{iv} in $\mathbf{PRF}_i'''$

Comment : PRF_{iu} is that PRF within $\mathbf{PRF}_i'''$ which minimizes obscuration within the priority 4 area.

Let $par4_i$ be a fourth pair of site adaptable parameters, and define the set $\mathbf{PRF}_i''''$ such that $\mathbf{PRF}_i'''' \subseteq \mathbf{PRF}_i'''$, and for any arbitrary PRF_{iw} in $\mathbf{PRF}_i''''$,

$$\mathbf{l}_i\ (PRF_{iw}) \leq min4_i + par4_i\ .$$

Comment : The set $\mathbf{PRF}_i''''$ is all PRFs within $\mathbf{PRF}_i''''$ whose obscured priority 4 area is within $par4_i$ km^2 of the minimum.

Let PRF_i be the optimal PRF values for regions 1 and 2, where PRF_i are elements of $\mathbf{PRF}_i''''$, respectively , and

$PRF_i \geq PRF_{ix}$ for any arbitrary PRF_{ix} in $\mathbf{PRF}_i''''$

Comment : PRF_i is the highest PRF value within the set $\mathbf{PRF}_i''''$

An example to illustrate the selection process appears as Fig. 3-1, using four hypothetical obscuration profiles.

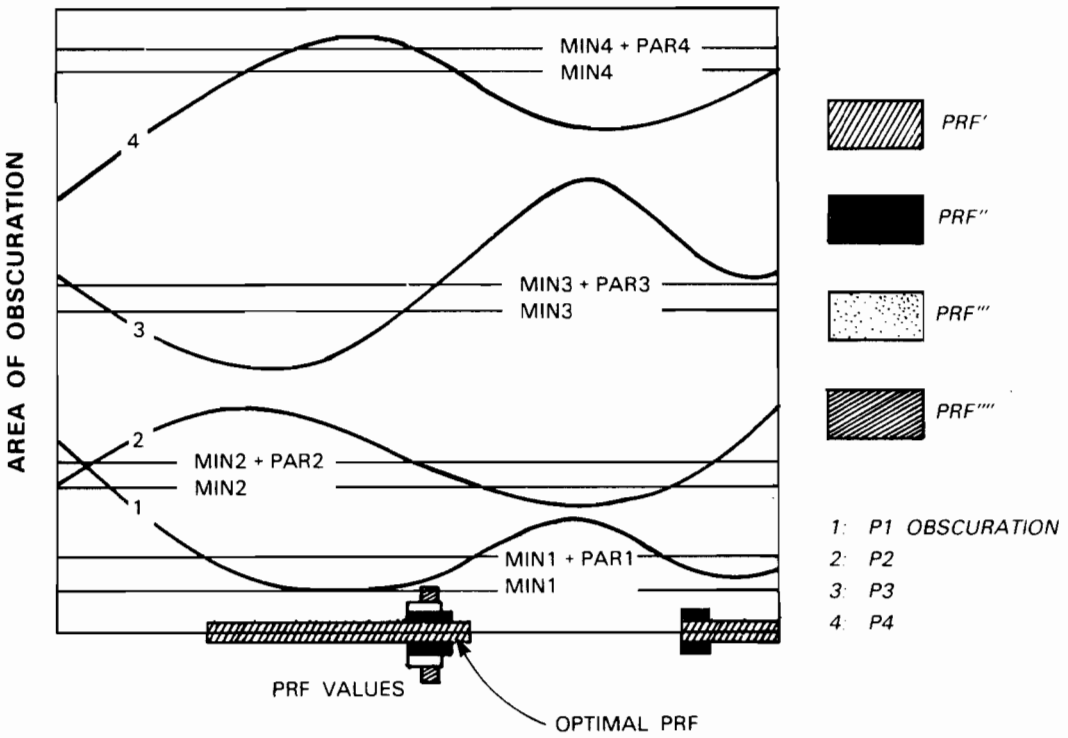

Figure 3-1. An example of the PRF selection criteria.

4.0 Sample Software Realization

4.1 Software Overview

An algorithm which automatically and adaptively selects PRF values has been implemented in software, and is undergoing real time tests at the FAA TDWR testbed radar. This testbed radar is currently located near the Stapleton International Airport in Denver, CO, and is being used to test and exercise various TDWR concepts and algorithms.

The first operational version of the PRF software was developed to minimize obscuration over the total hazardous weather identification region under investigation. The second version of this algorithm, which is currently operational at the radar site, was upgraded to include obscuration minimization over the Stapleton runways. The third version of the algorithm is under development and will incorporate obscuration avoidance over meteorologically defined regions; i.e., will minimize obscuration according to all criteria specified in Section 3. Plans call for this third and final version to be implemented at the testbed radar prior to the spring of 1988.

The algorithm was written in the FORTRAN 77 programming language, and consists of approximately 1000 executable lines of code. It cycles in real time at the radar site, and is capable of providing the PRF values used in routine data collection activities. It requires 1 to 3 CPU seconds on the real time site computer, a Concurrent model 3280, in order to process the data from the distant weather surveillance scan. The variation in CPU time is directly related to the amount of distant weather present, and thus the amount of obscuration assessment that must occur. The surveillance scan and subsequent PRF selection process are conducted approximately once every 5 minutes.

The top level flow diagram of the software appears as Fig. 4-1, where dotted lines indicate anticipated upgrades. The code was developed in a modular fashion to make upgrades easily accomplished.

4.2 TDWR Testbed Preliminaries

The TDWR testbed radar is S-Band, and with one exception, operates at PRFs between 700 and 1220 Hz. (The increased likelihood of radial velocity ambiguities at C-Band will undoubtedly require the TDWR system to operate at higher PRF values than are currently used by the testbed radar.) In support of the PRF algorithm, the testbed radar conducts a low elevation, full 360 deg, distant weather surveillance scan at a PRF of 350 Hz. This enables unambiguous range measurements out to a range of approximately 425 km. For the analysis which follows, it was assumed that the radar may operate at any integer valued PRF within the available set (700 to 1220 Hz), and selects the "optimal" accordingly. (The TDWR system is not required to provide this full repetoire of values, but rather to ensure that the available set provide the ability to move distant weather about within the region of interest in range increments of no greater than 3 km.)

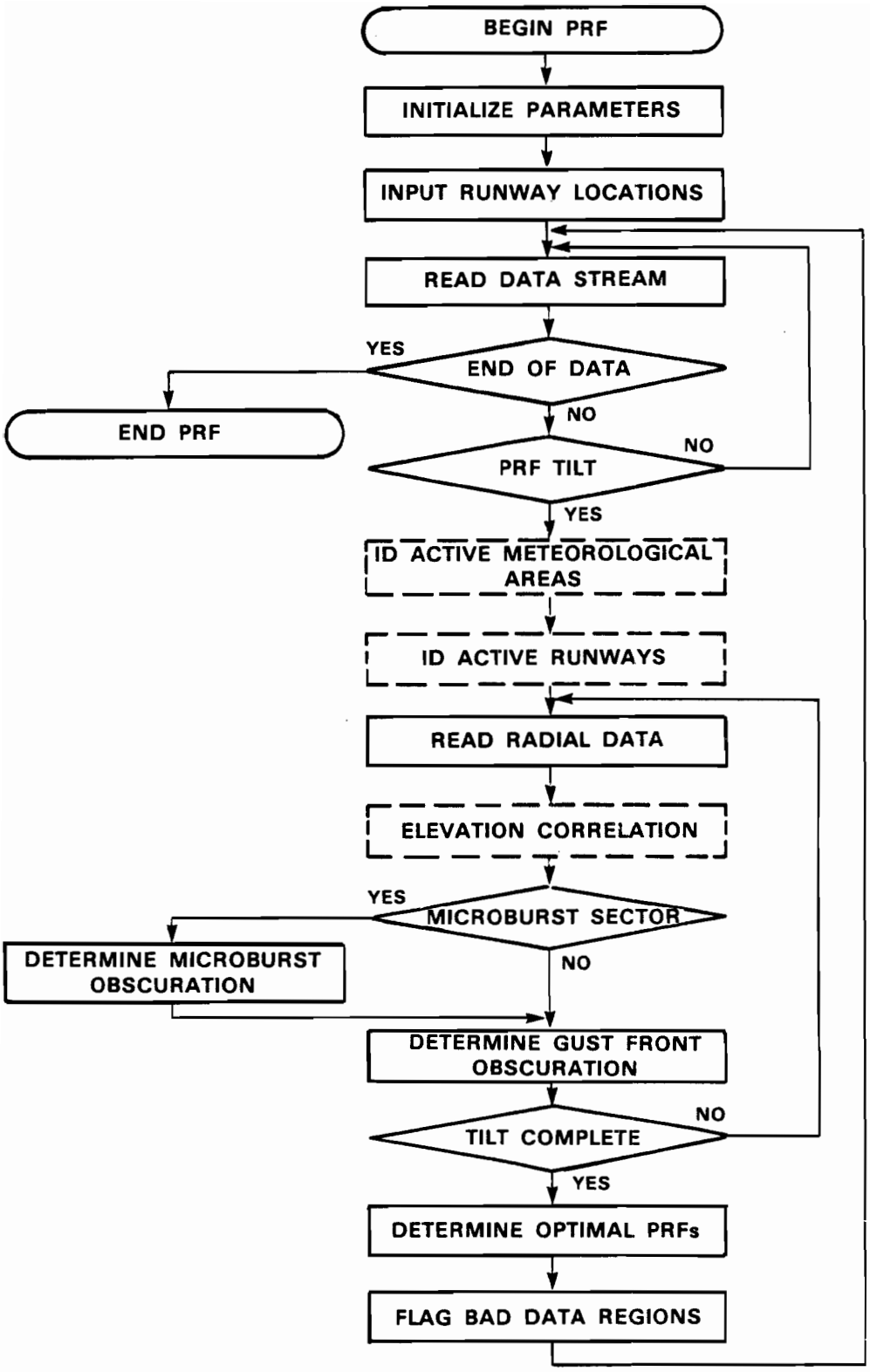

Figure 4-1. Top level flow diagram for PRF algorithm.

4.3 Performance Examples

Three examples of the performance of version 1 and one example of the performance of version 2 of this algorithm are presented in this report using data collected during the summer of 1987 at the Denver testbed site.

4.3.1 Case 1: 12-13 June 1987

From 1620 UT (universal time) on 12 June to 0128 UT on 13 June, 28 microbursts and 4 gust fronts were recorded by the testbed meteorologist and operators who were observing the real time radar displays. (Local Denver time is 6 hours less than universal time.) This early summer storm clearly represents the type of situation in which it is of utmost importance to ensure that the data being provided the meteorological algorithms are as free as possible from range aliased contamination. Otherwise, when humans are no longer in the loop, (as will be the case for TDWR operations) the fully automated detection of these hazardous weather events may not occur.

Figure 4-2 illustrates the changing distant weather situation over the course of the 12-13 June data gathering interval. (The strong reflectivity which is observed to the west of the radar site is attributed to clutter from the Rocky Mountains.) As can be seen, small storms began to form about the area. They increased in number and volume, and moved in an easterly direction. These small, isloated storms eventually merged into several concentrated masses that appear centered on the Kansas and Nebraska border, at a range of roughly 220 km from the radar site.

During the surveillance scan, the PRF algorithm examines all distant range cells. (For this analysis, a cell is defined to be a region 1-deg by 2-km.) If the signal strength within this cell surpasses a site-dependent threshold value, it is declared to be a distant weather cell, capable of causing in-trip range obscuration. For version 1 of the algorithm, those PRF values which would result in 2nd, 3rd, and possibly even 4th trip obscuration from this distant storm cell are calculated and subsequently recorded. After completing the surveillance scan, the number of obscured in-trip cells in the two hazardous weather identification regions for each PRF between 700 and 1220 Hz is available for further processing. (The gust front region is approximated as being within 70 km of the radar site, and contains roughly 12000 cells; the microburst region is approximated as being within a specified 120 deg sector, within 40 km of the radar site, and contains roughly 2000 cells.)

An example to illustrate obscuration assessment and PRF selection appears on page 17. Figures 4-3a, b and c are all enlargements of the storm region identified at time 01:06:49 UT in the lower right hand corner of Fig. 4-2. (This storm lies outside the sector which affects the microburst region; thus gust front PRF selection will be demonstrated in this example.) These three figures illustrate the portions of the distant storm that will fold into the gust front region on 2nd and 3rd trip for three PRF values. The obscuration profile for the gust front region which is computed by the PRF algorithm for this time is illustrated in Fig. 4-4. From the information contained in this profile, version 1 of the PRF algorithm selects that PRF value which minimizes (to within some epsilon) the number of obscured in-trip cells. For the example cited above, a PRF of 1066 Hz was selected for subsequent use. Referring to Fig. 4-4, a 1066 Hz PRF will result in approximately 225 obscured cells. These are illustrated in the obscuration map (Fig. 4-5)

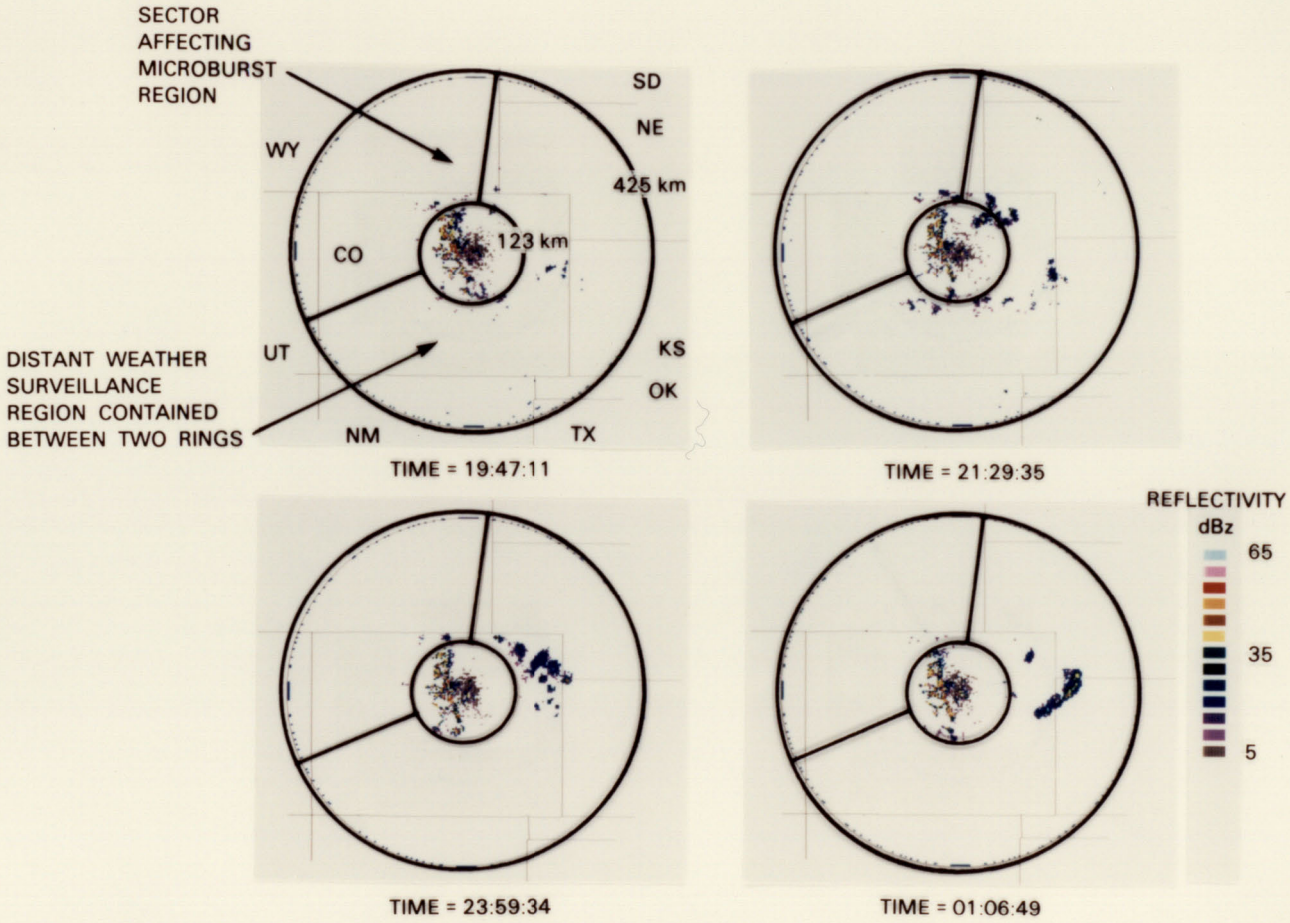

Figure 4-2. Reflectivity profiles of 12 to 13 June 1987.

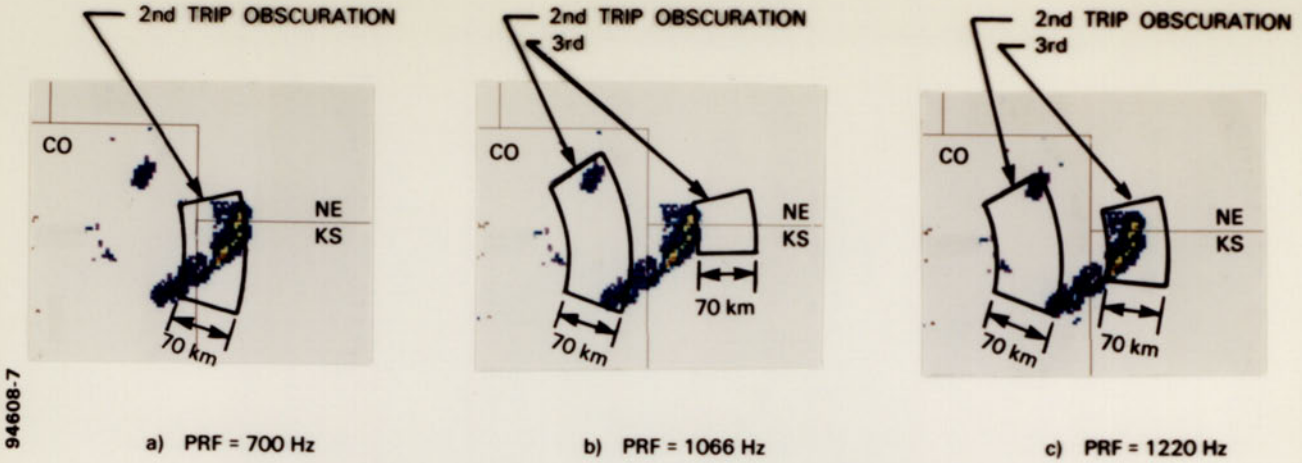

Figure 4-3. Obscuration assessment at 0107 UT.

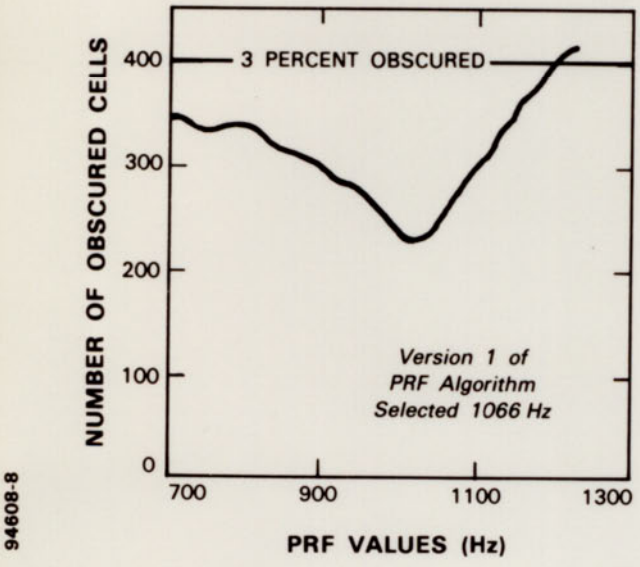

Figure 4-4. Gust front obscuration profile at 0107 UT.

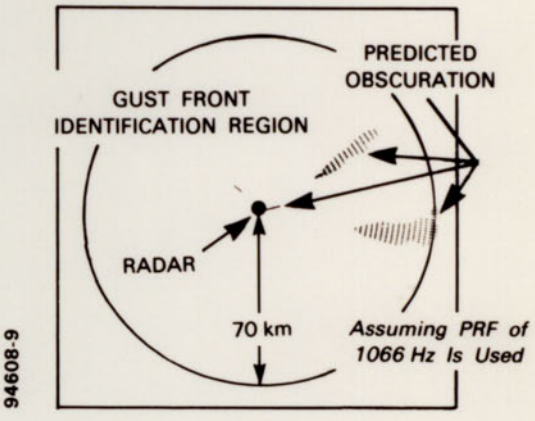

Figure 4-5. Predicted gust front obscuration at 0107 UT.

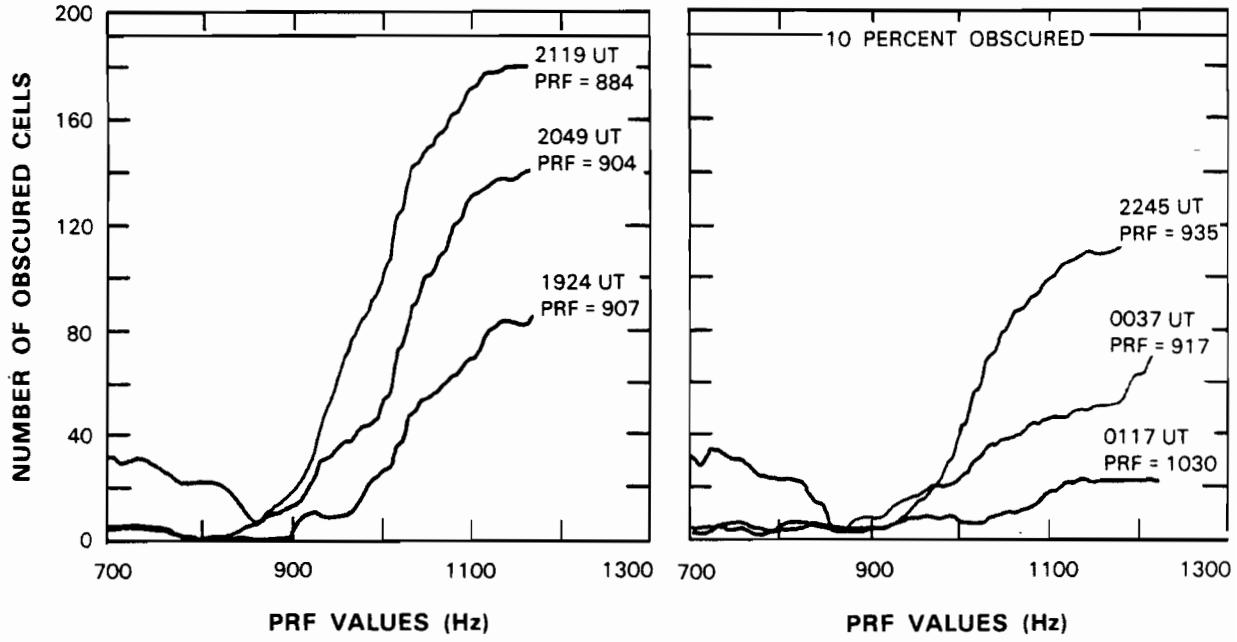

a) MICROBURST OBSCURATION PROFILES

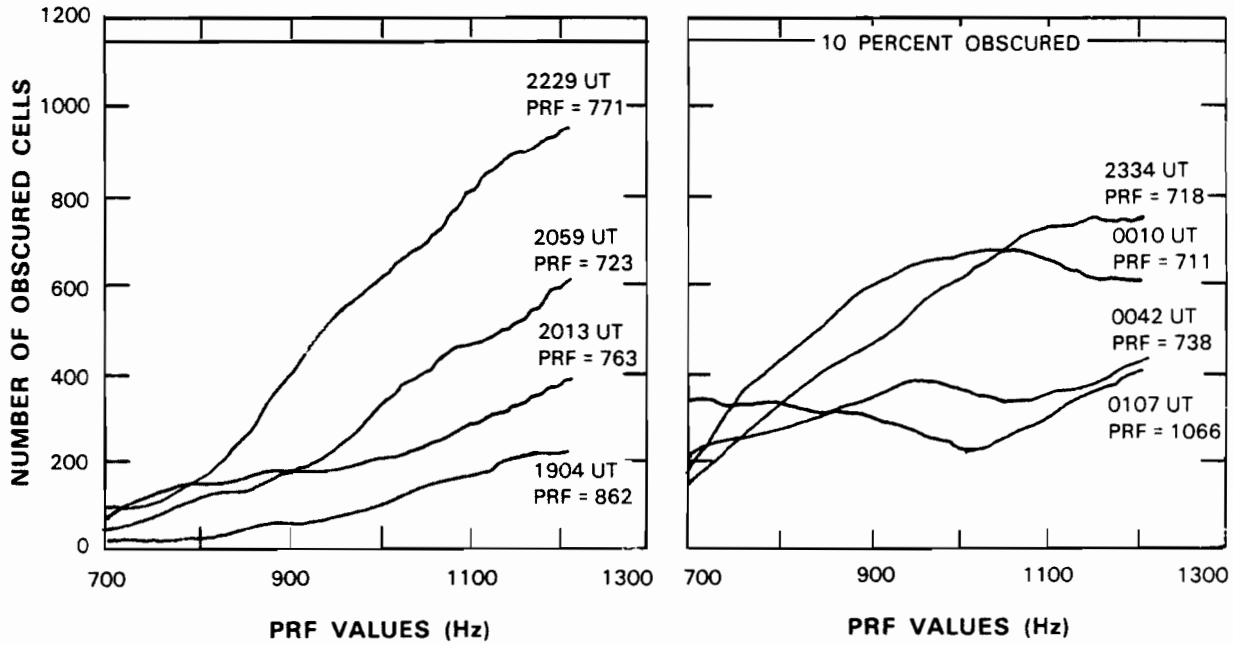

94608-10

b) GUST FRONT OBSCURATION PROFILES

Figure 4-6. Obscuration profiles of 12 to 13 June 1987.

which is the final output of the PRF algorithm at the time in question. This obscuration information is in complete agreement with the situation presented in Fig. 4-3b.

For completeness, Figs. 4-6a and b illustrate sample obscuration profiles for the microburst and gust front regions, respectively, over the course of the 12-13 June data gathering interval. The times and the PRF values which were selected by version 1 of the PRF algorithm are identified on each profile.

4.3.2 Case 2: 2-3 July 1987

On 2 July 1987, a storm of mesoscale proportion developed around the Denver area. 17 microbursts, 4 gust fronts, and a tornado were detected on the real time radar displays by the site personnel. (In addition, several of these hazardous weather events were visually spotted by the team.) The data gathering interval lasted from 1854 UT (July 2) to 0436 UT (July 3). Examples of the reflectivity profiles for the duration of this data gathering interval appear in Fig. 4-7.

Sample obscuration profiles for the 2-3 July event for both the microburst and gust front regions are shown in Figs. 4-8a and b, respectively. These profiles clearly illustrate the evolution of the storm. The earlier profiles show only a minimal level of obscuration as the storm is forming. As time progresses and the storm builds, the obscuration profiles likewise build. The storm eventually passes outside that area which would cause obscuration to the microburst region; a fact which is reflected as the microburst obscuration profiles are seen to subside. The storm remains, however, within the area affecting the gust front region throughout the duration of the data gathering interval.

As seen in Fig. 4-8b, at approximately 0118 UT, a PRF of 708 Hz was selected for use within the gust front identification region. (The prevailing distant weather situation at the time in question appears in the lower right hand corner of Fig. 4-7.) As seen in the 0118 UT obscuration profile, obscuration increases almost linearly with PRF value. Figures 4-9a and b illustrate obscuration assessment at the two PRF extremes; i.e., when obscuration is minimized (near 708 Hz) and when obscuration is maximized (at 1220 Hz). Approximately 500 cells are predicted to be obscured when the 708 Hz PRF is used. This obscuration is identified in Fig. 4-10, and is clearly supported by the information presented in Fig. 4-9a.

4.3.3 Case 3: 15 August 1987

No hazardous wind shear events were detected during the data gathering activities of 15 August. Much time was spent at the testbed site on that day, however, checking out and verifying the output from the PRF algorithm. This day was therefore selected for inclusion in this report.

Figure 4-11 illustrates the distant weather situation which existed on 15 August. Typical of storm activity around the Denver area, small storm cells began to develop to the northwest of the testbed site. These cells gradually increased in strength and drifted to the east. Figure 4-12a and b illustrate examples of the obsuration profiles for this day for the microburst and gust front regions, respectively.

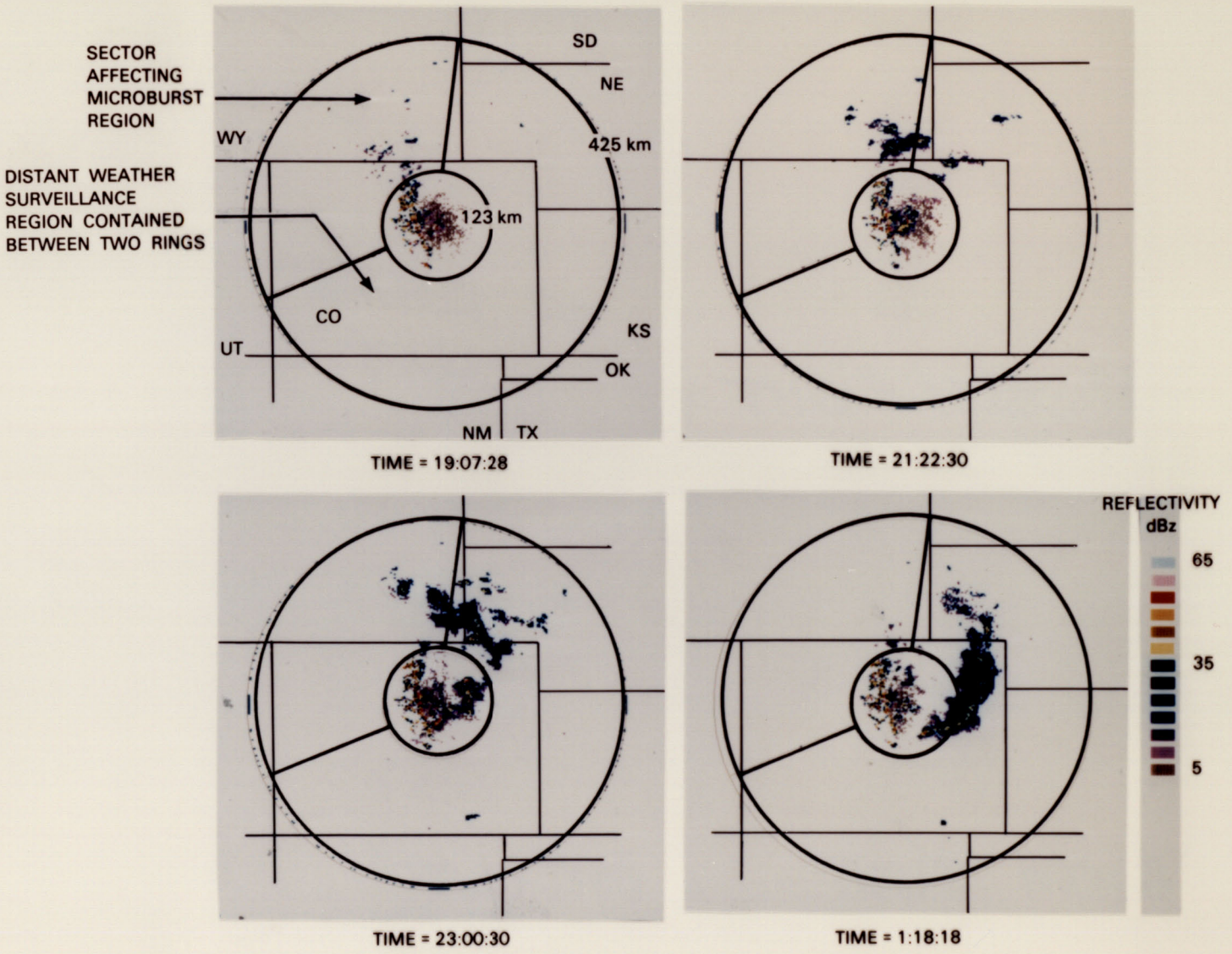

Figure 4-7. Reflectivity profiles of 2 to 3 July 1987.

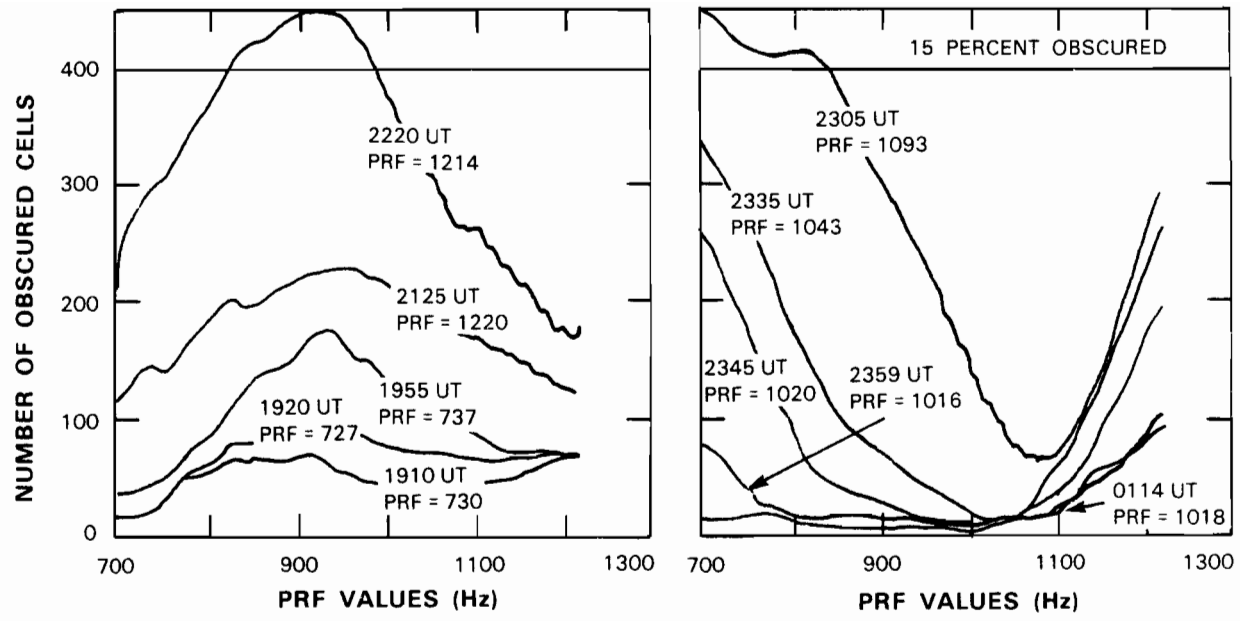

a) MICROBURST OBSCURATION PROFILES

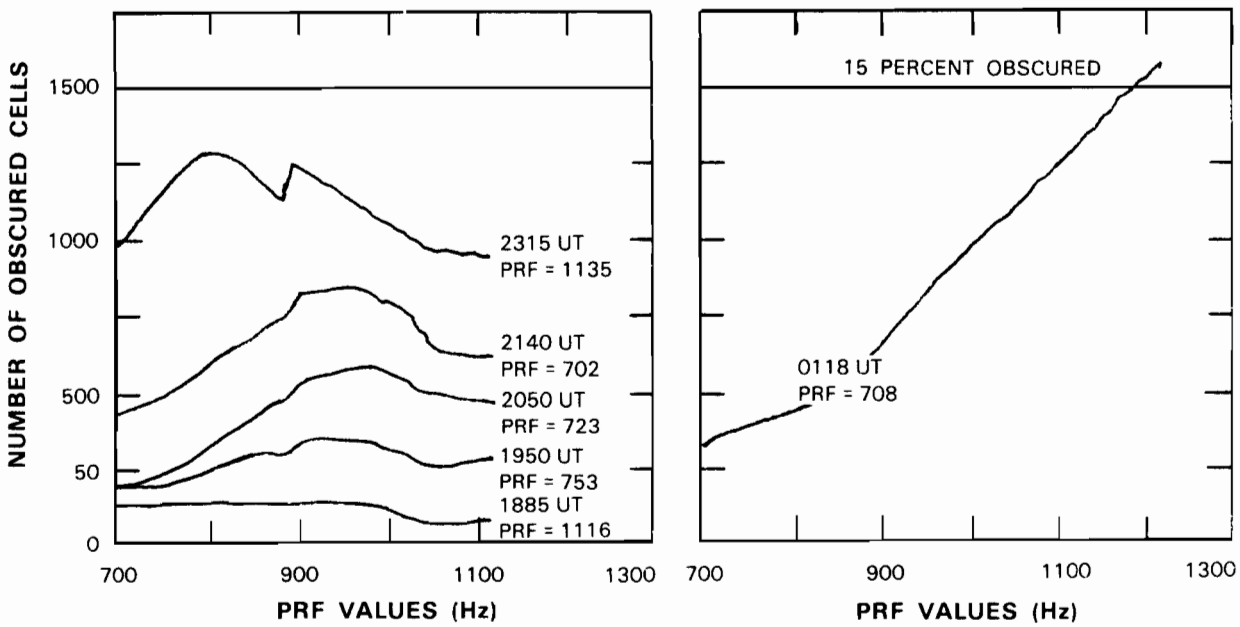

b) GUST FRONT OBSCURATION PROFILES

94608-12

Figure 4-8. Obscuration profiles of 2 to 3 July 1987.

94608-13

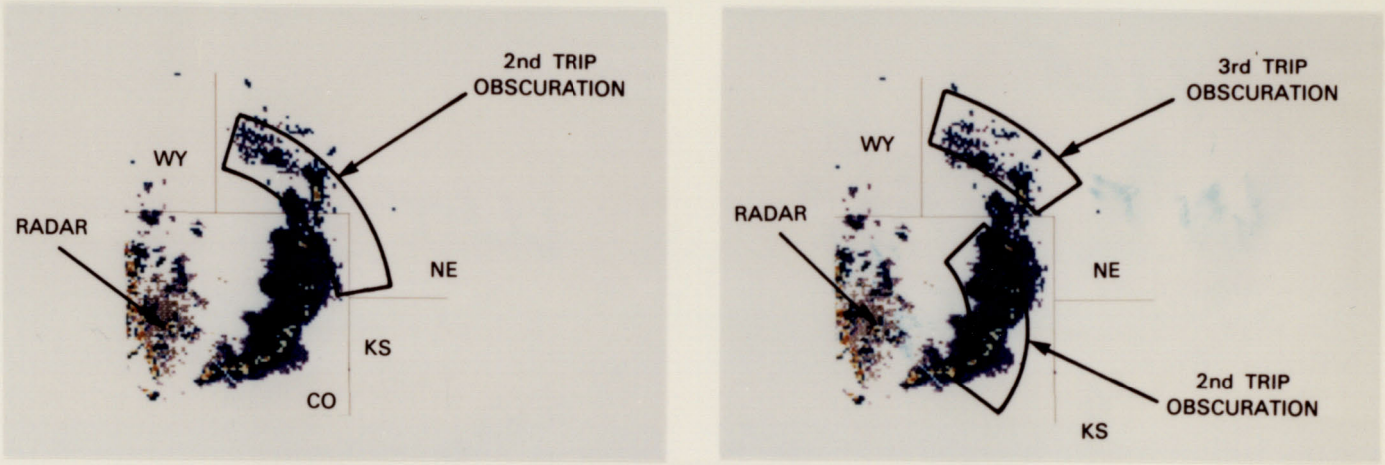

Figure 4-9. Obscuration assessment at 0118 UT.

94608-14

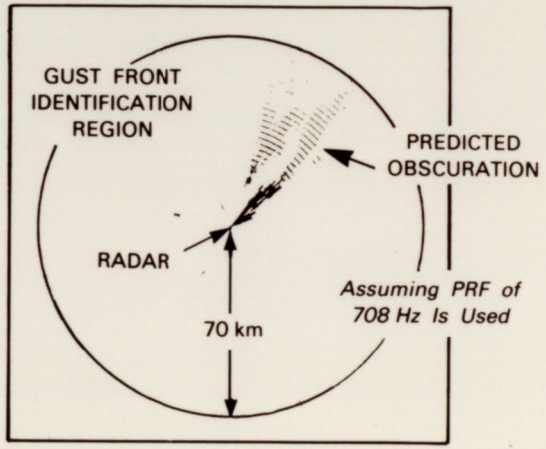

Figure 4-10. Predicted gust front obscuration at 0118 UT.

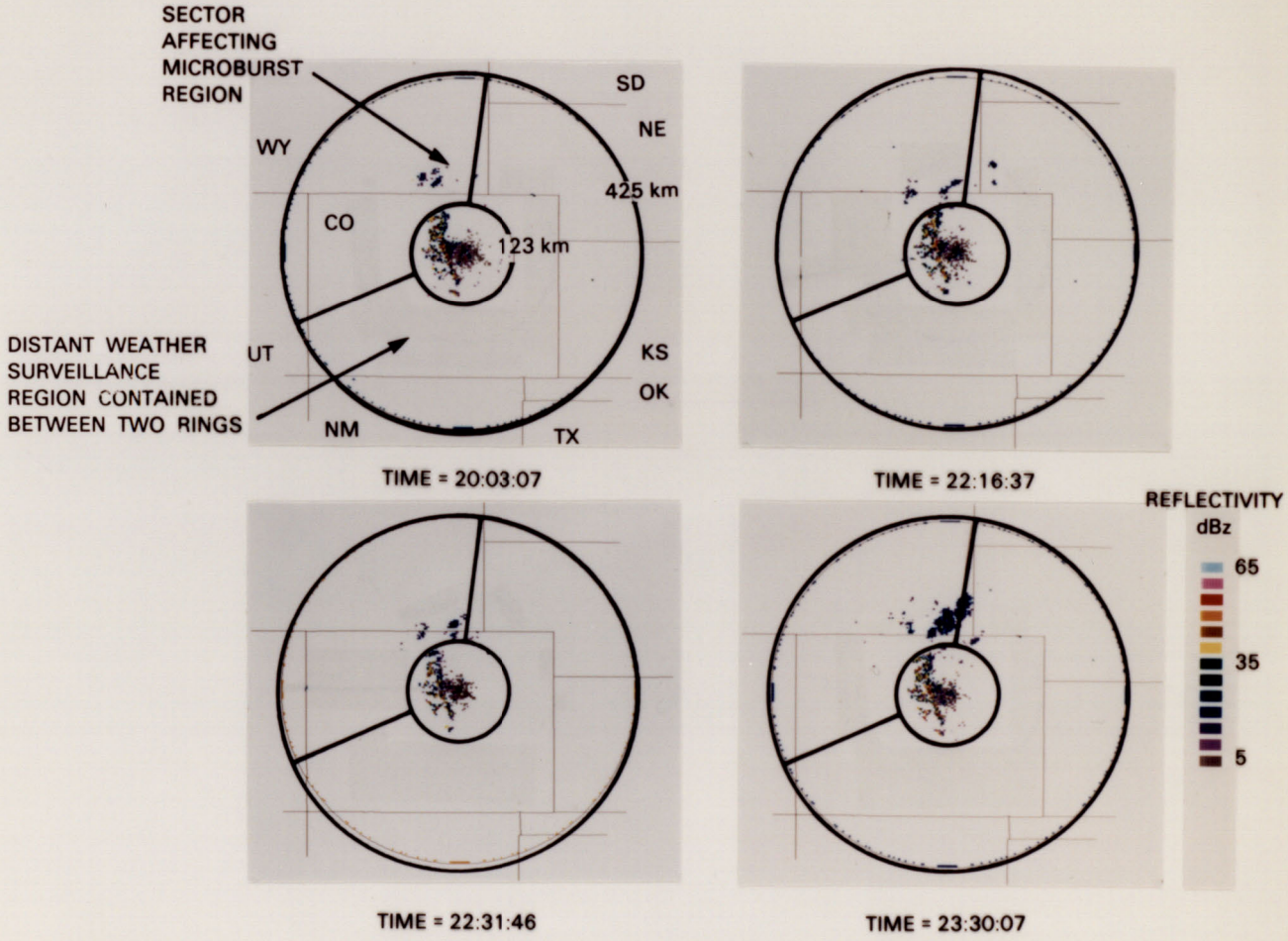

Figure 4-11. Reflectivity profiles of 15 August 1987.

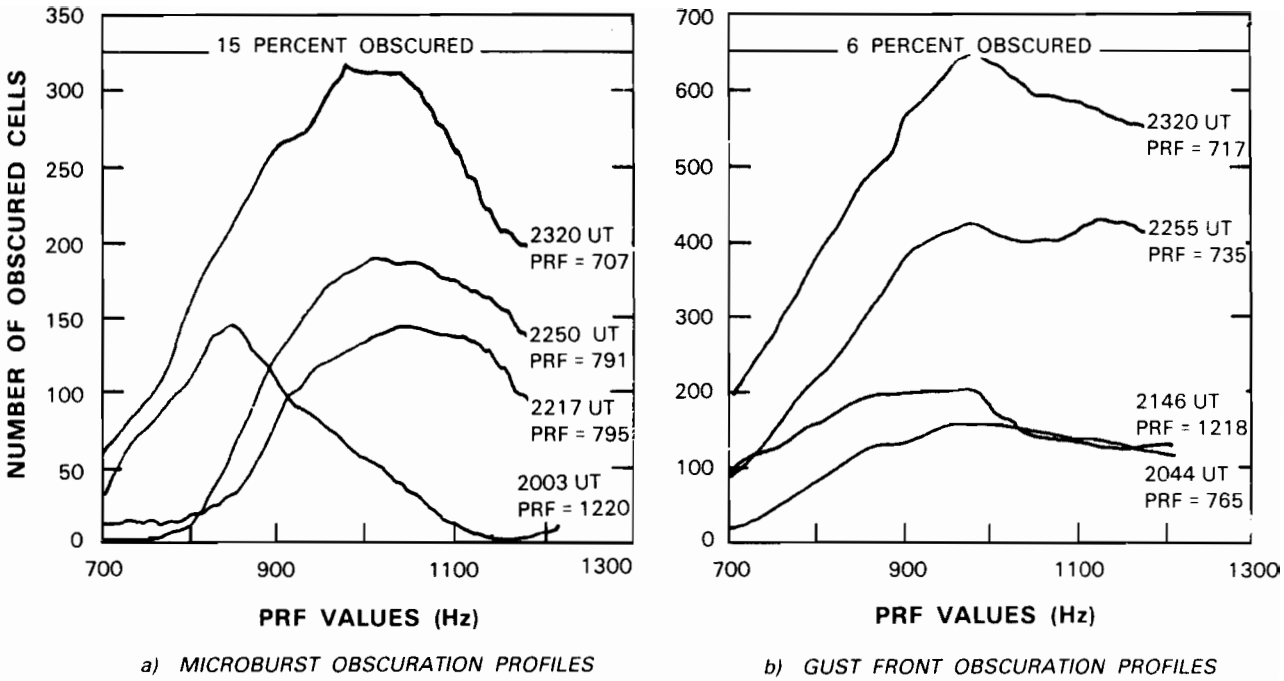

Figure 4-12. Obscuration profiles of 15 August 1987.

94608-17

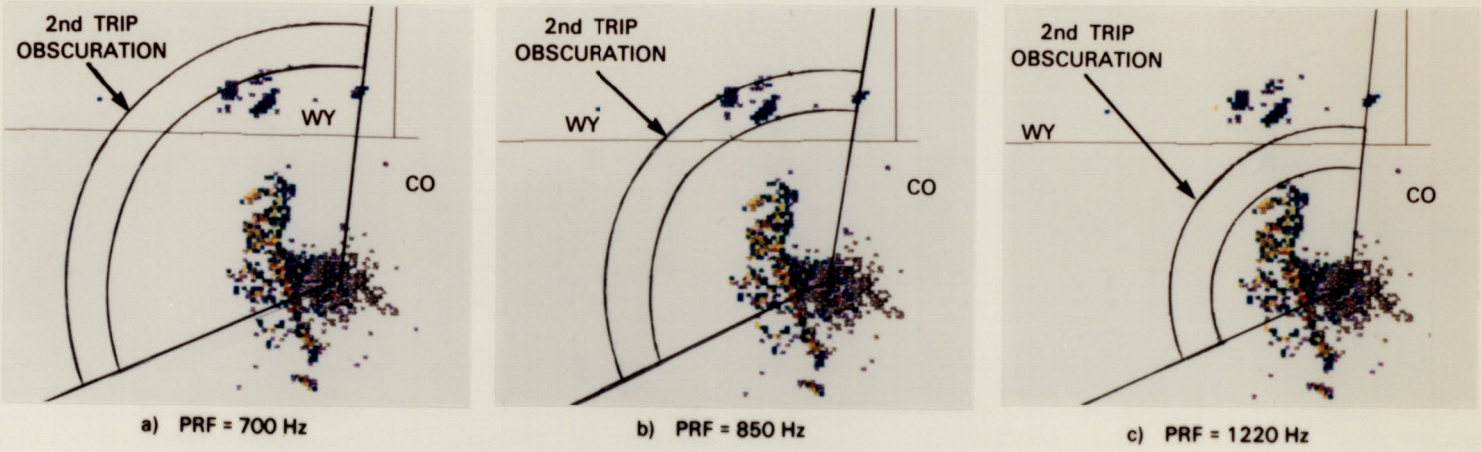

Figure 4-13. Obscuration assessment at 2003 UT.

94608-18

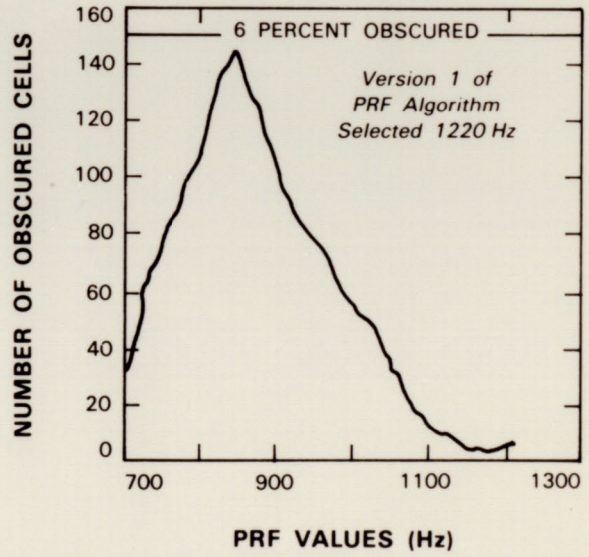

Figure 4-14. Microburst obscuration profile at 2003 UT.

Obscuration assessment at time 2003 UT for the microburst region is illustrated on page 25. The prevailing distant weather situation at this time appears in the upper left hand corner of Fig. 4-11, and three enlargements of the storm region at this time appear as Figs. 4-13a, b, and c. As can be seen, only a small portion of this storm would fold into the microburst identification region if a PRF of 700 Hz were used. The entire storm would obscure the region if a PRF of 850 Hz were used. Negligible obscuration would exist if a PRF of 1220 Hz were used. This information is clearly reflected in the obscuration profile, Fig. 4-14, which is computed by the PRF algorithm. (Version 1 of the algorithm selects 1220 Hz as the "optimal" PRF.)

4.3.4 Case 4: 4 September 1987

Version 2 of the PRF selection algorithm treats obscuration minimization specifically over the Stapleton runways, in addition to obscuration minimization over the general region under investigation. Version 2 was recently implemented at the testbed site, and data which were collected on 4 September were selected to illustrate sample output from this upgraded version. Figure 4-15 illustrates the distant weather situation over the course of 4 September. 5 microbursts and 3 gust fronts were recorded by testbed personnel to have occurred in the vicinity of the radar on that day.

At the completion of the surveillance scan, version 2 of the algorithm computes two obscuration profiles for each region. The first profile identifies specific obscuration over the Stapleton runways as a function of PRF value, and the second identifies general obscuration within the region as a function of PRF value. Examples of these profiles and the subsequent PRF selection from these profiles appear on the following pages. (Profiles labelled A denote obscuration over the Stapleton runways (and 3 mi beyond), and profiles labelled B denote obscuration over the general region under investigation.)

In a manner similar to that introduced in Section 3, the PRF algorithm first determines an "acceptable subset" of PRF values. Since it is of higher priority to minimize obscuration over the runways, this subset of PRF values is that which results in minimal levels of obscuration specifically over the runways. The general obscuration which is associated with this subset of PRF values is then examined. Those PRFs within the first subset which result in minimal levels of profile B obscuration are determined, thus forming a revised "acceptable subset". The highest possible PRF value within this revised set is chosen for subsequent use.

Figure 4-16 illustrates the distant weather situation on 4 September at time 1849 UT. Figure 4-17 details PRF selection for the microburst region at this time and presents the predicted obscuration map. Figure 4-18 is a similar exercise for the gust front region. Figures 4-19 through 4-21 duplicate the events that were illustrated above at another instant in time (2022 UT).

The PRF values that are produced by the algorithm are automatically used during subsequent scans at the testbed radar site. Data collected on these subsequent scans can therefore be used to verify that the predicted obscuration did indeed occur. This final step completes the algorithm verification. Figure 4-22 illustrates the reflectivity and radial velocity data that were recorded in the gust front identification region when the selected PRF was used. The distinctive long and narrow signature of the range aliased echoes are seen to occur as predicted.

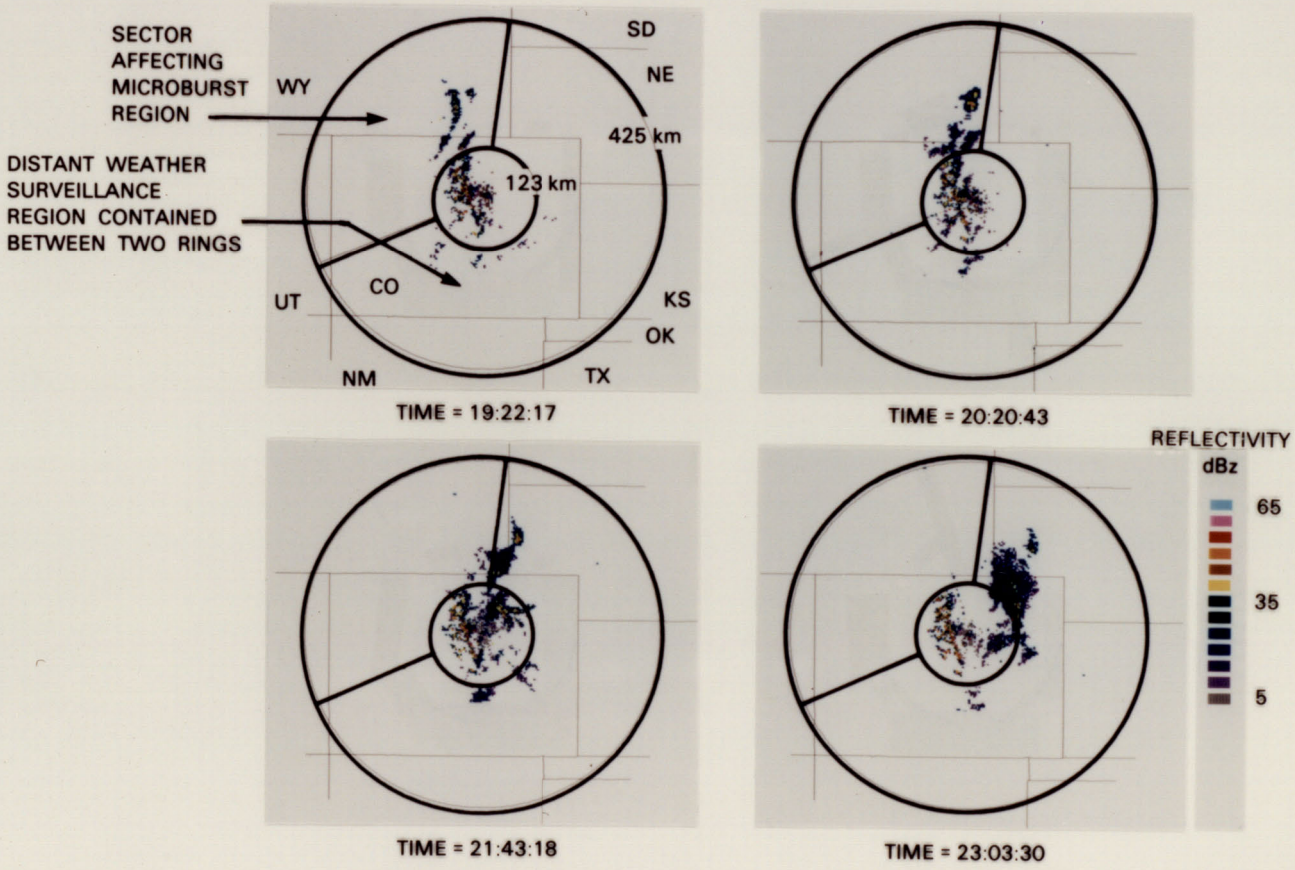

Figure 4-15. Reflectivity profiles of 4 September 1987.

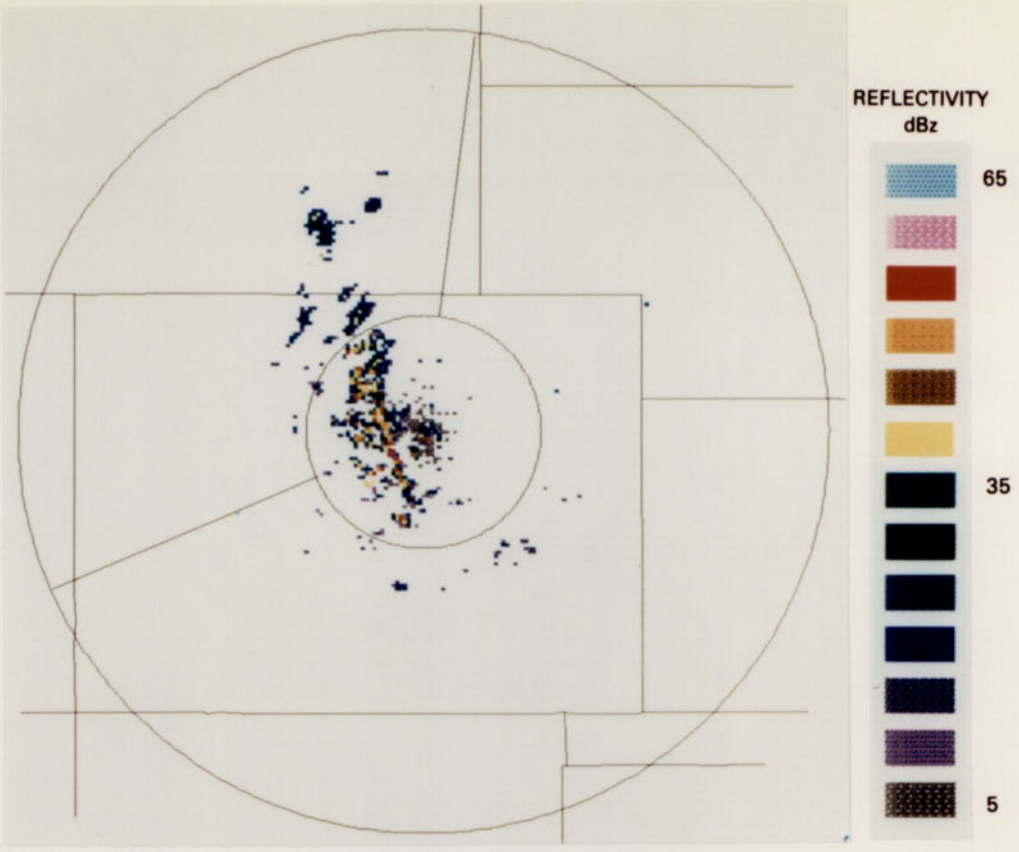

94608-20

Figure 4-16. Distant weather at 1849 UT.

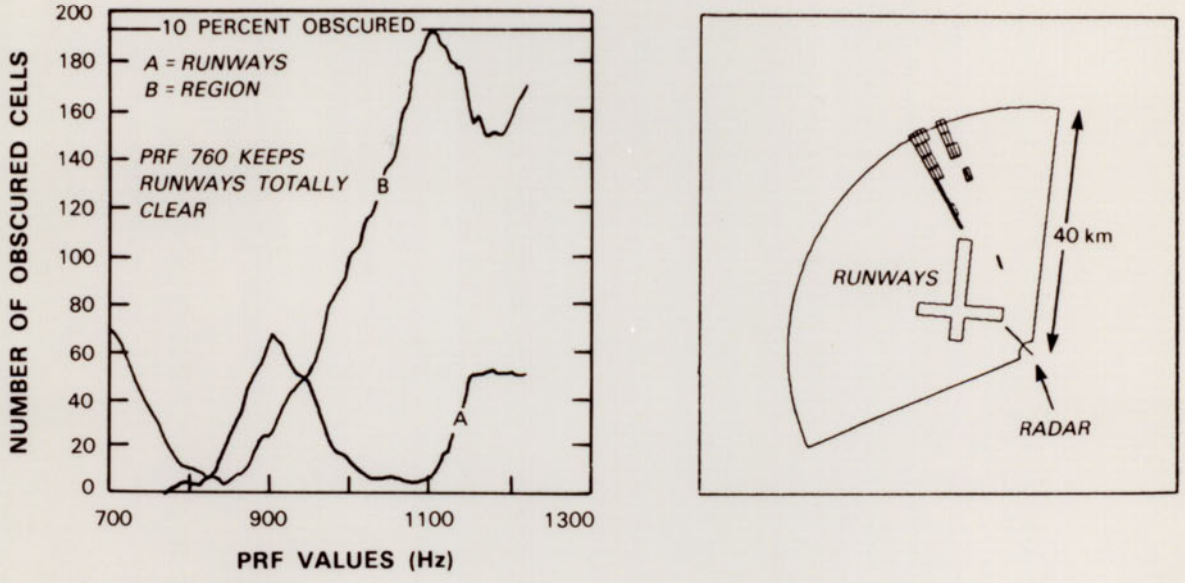

94608-21

a) OBSCURATION PROFILES

b) OBSCURATION MAP

Figure 4-17. Microburst region obscuration assessment at 1849 UT.

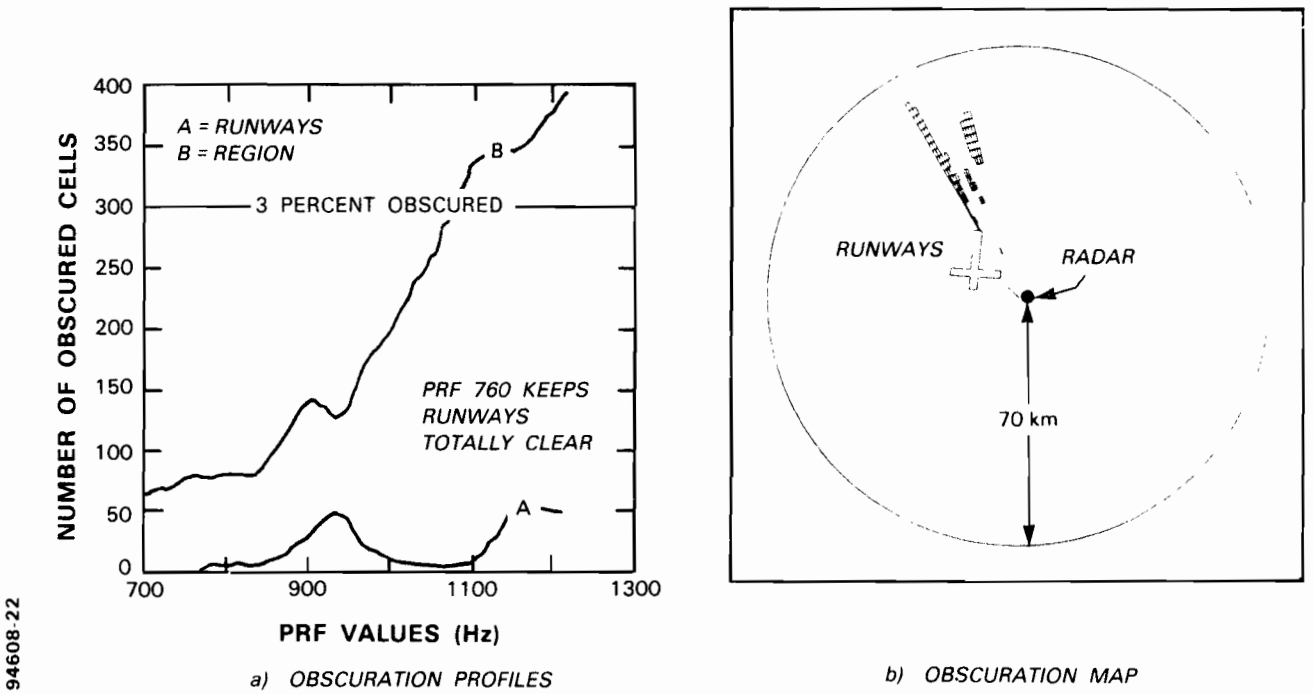

Figure 4-18. Gust front region obscuration assessment at 1849 UT.

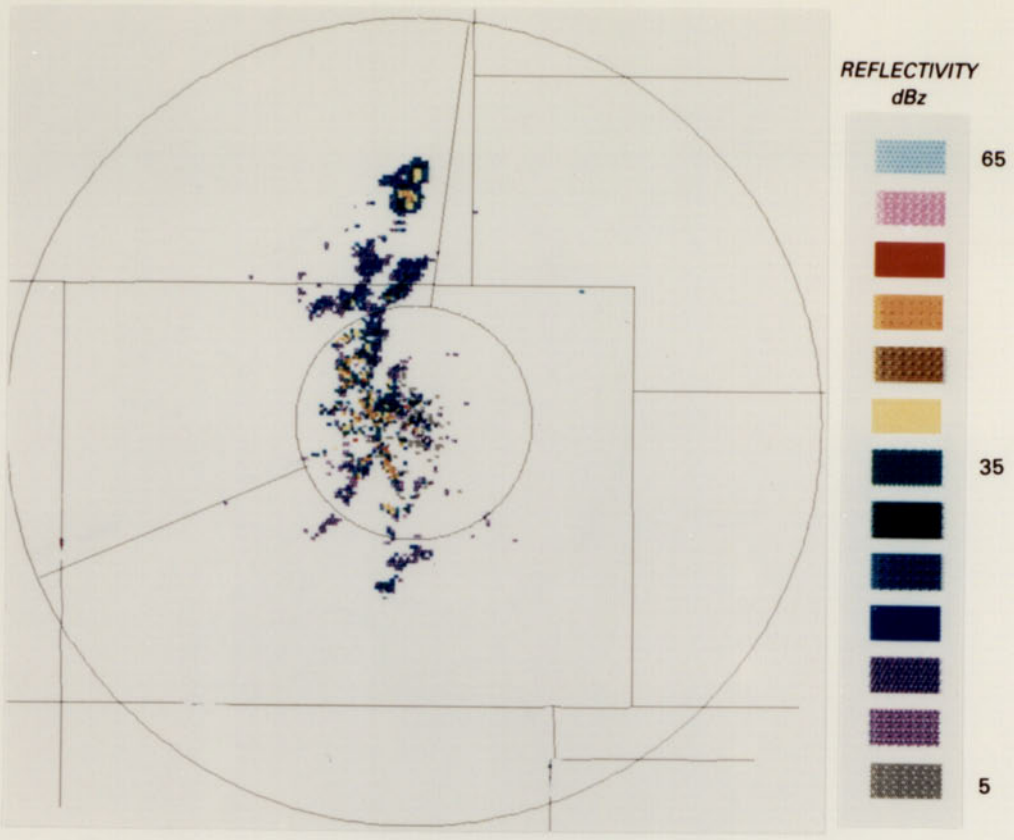

94608-23

Figure 4-19. Distant weather at time 2021 UT.

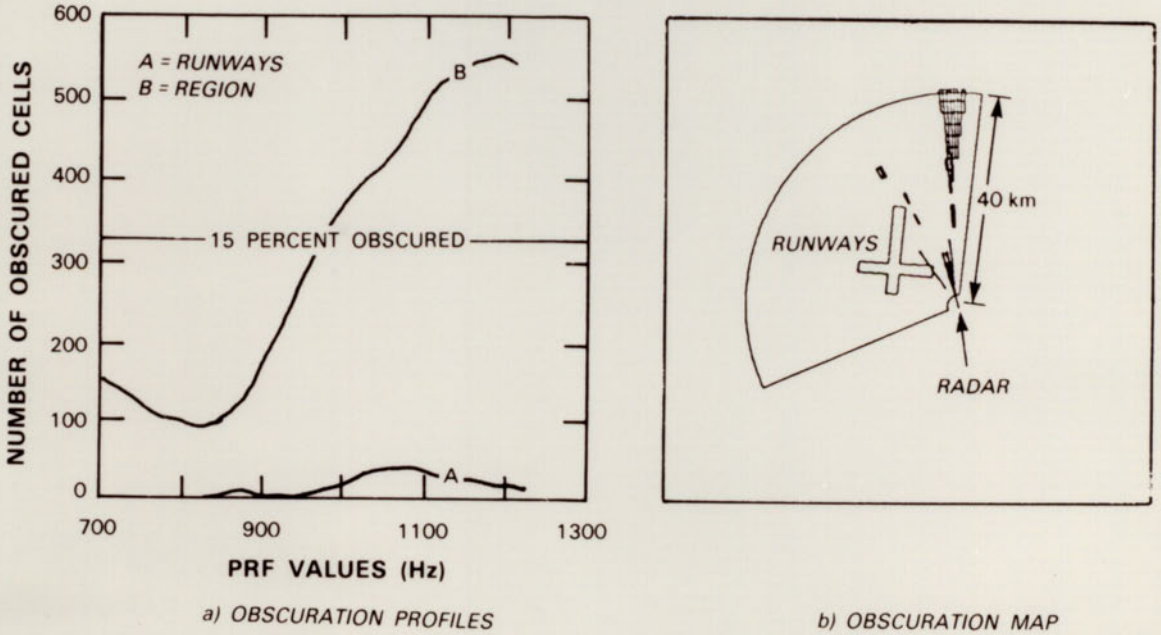

94608-24

a) OBSCURATION PROFILES

b) OBSCURATION MAP

Figure 4-20. Microburst region obscuration assessment at 2021 UT.

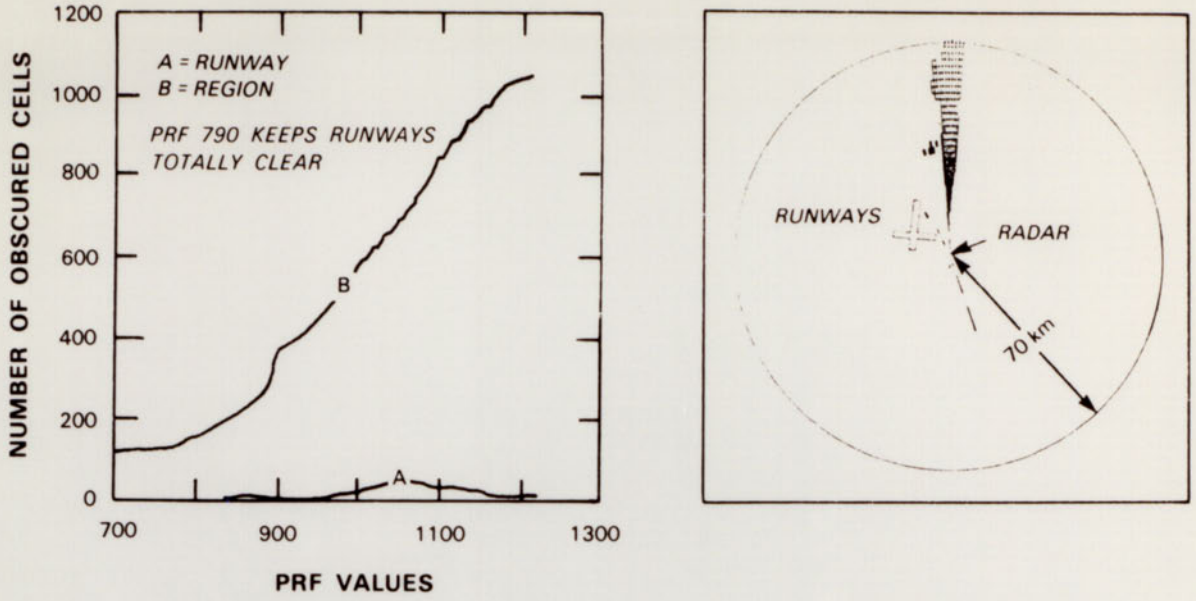

94608-25

a) OBSCURATION PROFILES

b) OBSCURATION MAP

Figure 4-21. Gust front region obscuration assessment at 2021 UT.

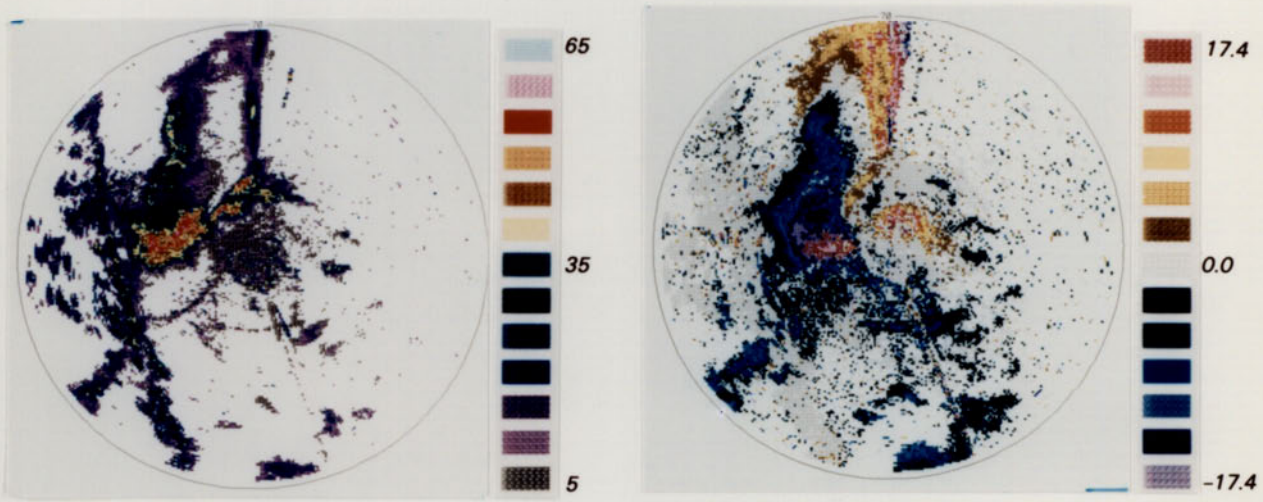

94608-26

a) REFLECTIVITY (dBz)

b) RADIAL VELOCITY (m/s)

Figure 4-22. Range aliased returns at 2023 UT.

5.0 Conclusion

The future Terminal Doppler Weather Radar system shall automatically identify hazardous weather phenomena near high traffic airport regions. The TDWR system must ensure that the data used as input to the identification algorithms are of highest possible quality. Obscuration due to ambiguous range foldover from distant weather can seriously degrade the quality of Doppler weather radar data. The TDWR system must therefore make provisions by which to minimize the amount of range obscuration due to distant weather.

The specification for the TDWR system calls for adaptive and selective PRF pocedures as the means by which to minimize obscuration due to ambiguous range foldover. The procedures and the criteria for the selection of PRF in order to accomplish this task have been specified herein. Procedures have been defined by which to identify distant weather, assess obscuration which would be attributed to this distant weather as a function of PRF value, select that PRF which minimizes obscuration according to specified criteria, and finally, provide a means by which to flag any regions of anticipated obscuration.

This document demonstrates that range obscuration for a Doppler weather radar can be minimized in real time exercises according to the procedures specified above. An algorithm is being developed to satisfy minimization objectives, and is currently undergoing real time tests at the TDWR testbed radar in Denver, CO. This algorithm was introduced in this document, as were examples of its performance during a variety of data gathering exercises conducted during the summer of 1987.

Appendix A Distant Weather Considerations

Appendix A of this report is to develop the TDWR requirement which specifies that reflectivity measurements be obtained out to a maximum range of 460 km. This requirement supports the PRF selection algorithm during the distant weather identification portion of the analysis. Within the context of this report, 460 km bounds the furthest range extent which must be examined for the occurrence of distant weather. As will be developed, this value has theoretical justification as well as operational justification.

Reflectivity measurements out to the 460 km maximum range will be made during the distant weather surveillance scan. These measurements are made in order to characterize the prevailing distant weather situation. The scan itself is conducted at a low elevation angle (on the order of 1 deg). Due to the curvature of the earth, a constant elevation scan will observe storms at varying altitudes along the ray path. This is illustrated in Figure A-1, from [5]. Here, height above the surface is shown as a function of Earth arc distance, with ray paths illustrated for a variety of elevation angles. (Refractive effects due to the atmosphere have been included in the derivation of these plots.)

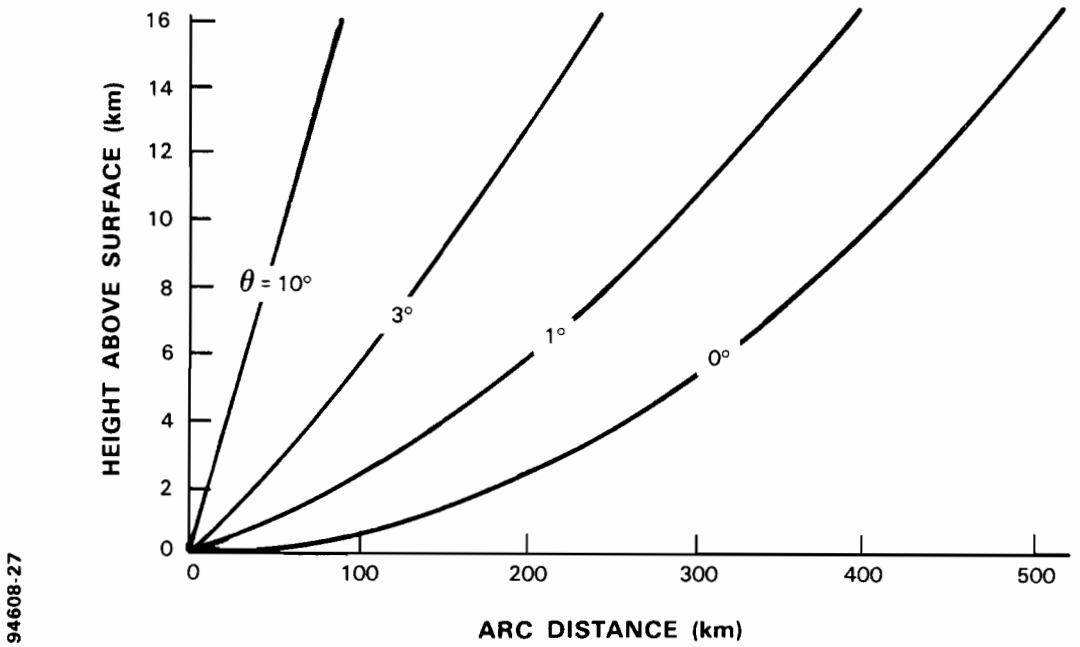

Figure A-1. Arc distance vs altitude.

Characteristics of storms which may be observed as distant weather are then examined to determine what types of storms will be observed along the ray path of the radar. In [6], the altitude and reflectivity profiles of six classses of storms of varying intensity are examined over time, with class 1 being a simple summer rainshower and class 6 being a thunderstorm of tornadic proportion. Figure A-2, from [6], succinctly illustrates some of the findings of that report. Here, typical growth patterns of the various classes of storms are seen to evolve over time. (As further discussed in [6], the altitude characteristics of this profile are expected to vary somewhat for different geographic locations.)

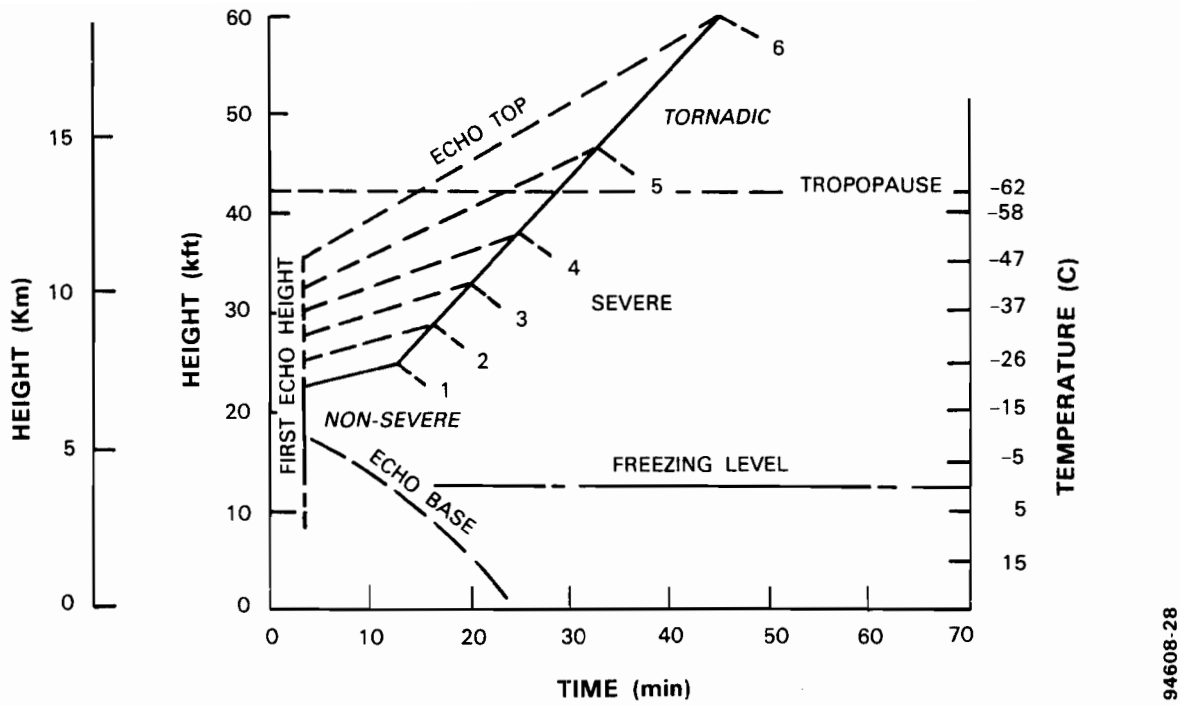

Figure A-2. Growth patterns of storms of varying intensity.

By combining information in the previous two plots, characteristics of weather which may be observed at different ranges from the radar can be determined. Of particular interest is any significant storm which may be located beyond 460 km, yet which attains an altitude to cause its echo to be returned to the radar. That storm would thus appear range aliased, even using the maximum unambiguous data gathering interval. This, of course, is the situation to be avoided. As can be seen, storms other than the most severe (i.e., class 6) which are located beyond 460 km are not expected to be visible using a surveillane scan which is placed at the horizon, covering from 0.0 deg to 0.5 deg in elevation. These are assumed to be adequately covered, and attention turns to a storm of supercell proportion, i.e., class 6. It is conceivable, based on these two plots alone, that such a storm, located just beyond 460 km from the radar could result in some obscuration during the surveillance mode of operation.

The rationale for the 460 km maximum unambiguous range follows. First, figure A-1 was generated assuming "perfect" conditions; i.e., no blockage due to terrain or structural buildings. Mountains, hills, minor variations in the terrain, and even simple obstructions will operationally reduce this visibility profile. As identified above, storms whose echo height surpasses an altitude of approximately 14 km may potentially cause obscuration during the surveillance scan. As was investigated in [7], the probability of occurrence of storms whose echo height surpasses this altitude is low. (Storms rarely ascend above the tropopause.) Figure A-3, from that report, illustrates the percentage of storm cells which attain the various altitudes shown, regardless of reflectivity. Even considering geographical variations in storm characteristics, one can conclude that the probability for such an

occurrence is less that 5%. To determine the probability that such a storm would subsequently cause obscuration during the surveillance scan, this storm is further required to be located precisely between 460 km and say 500 km from the radar. This conditionality requirement further reduces the probability of obscuration from such a storm.

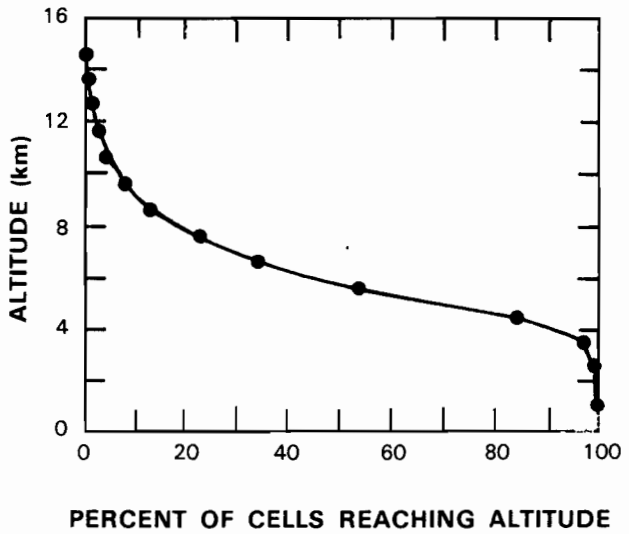

Figure A-3. Percent of cells reaching an altitude.

Two final arguments are presented to support the contention that the probability of obscuration by storms beyond 460 km is extremely unlikely. The reflectivity effects of such a storm would be reduced by nearly 30 dBZ due to range dependencies in the reflectivity calculation, hence the 50 dBZ distant storm cell would appear in-trip as 20 dBZ. A storm which may be on the order of 10 km in diameter and located at a range just beyond 460 km would cause in-trip obscuration to approximately 1 radial of data, and this represents a very small fraction of the total area under investigation.

Ray propagation paths, storm characteristics, and arguments to justify a maximum unambiguous range of 460 km were presented above. As important as all of the above discussion, however, is the operational experience in the observance of distant weather by radars. Indications [8] are that NSSL personnel are unaware of obscuration effects from any storms beyond 460 km; likewise, NWS radars have been unaffected by such phenomena. The FAA testbed radar in Denver has not observed any storms beyond its 429 km maximum unambiguous range limit. As a final argument for this value, the maximum unambiguous range for the NEXRAD system has also been specified at 460 km [9].

ACKNOWLEDGMENT

The author wishes to acknowledge the excellent work performed by Linda B. Garant, who has recently joined the TDWR range obscuration mitigation effort.

REFERENCES

[1] Skolnick, M.I, "Introduction to Radar Systems", 2nd Edition, McGraw-Hill Inc., New York, 1980.

[2] Terminal Doppler Weather Radar Specification, U.S. Department of Transportation, Federal Aviation Administration, FAA-E-2806.

[3] Campbell, S.D., "Terminal Doppler Weather Radar Siting Issues", M.I.T. Lincoln Laboratory, 43PM-WX-0005, 27 January 1987.

[4] Campbell, S.D. and Merritt, M.W. , "TDWR Scan Strategy Requirements", M.I.T. Lincoln Laboratory Project Report ATC-144, FAA Technical Report DOT/FAA/PM-87-25.

[5] Doviak, R.J. and Zrnic, D.S., "Doppler Radar and Weather Observations", Academic Press, Inc., Orlando, FL, 1984.

[6] Wilk, K.E., and Dooley, J.T., "FAA Radars and their Display of Severe Weather (Thunderstorms)", Technical Report # FAA-RD-80-65, National Severe Storms Laboratory, Environmental Research Laboratories, National Oceanic and Atmospheric Adminstration, July 1980.

[7] Konrad, T.G., "Statistical Models of Summer Rainshowers Derived from Fine-Scale Radar Observations", Journal of Applied Meteorology, Volume 17, February 1978, 171-188.

[8] Personal communication between J. Evans and K. Wilk.

[9] NEXRAD Technical Requirements, R4000-SP301, NEXRAD Joint Systems Program Office, Silver Spring, Md., 1 January 1986.